AD-A193 368 ON THE DYNAMICS OF THE AURORAL IONOSPHERE DURING THE BREAKUP OF A SUBSTORM(U) NORTHEASTERN UNIV BOSTON MA M B SILEVITCH 01 MAR 88 AFGL-TR-88-0020 1/1

UNCLASSIFIED F19628-83-K-0014 F/G 4/1 NL

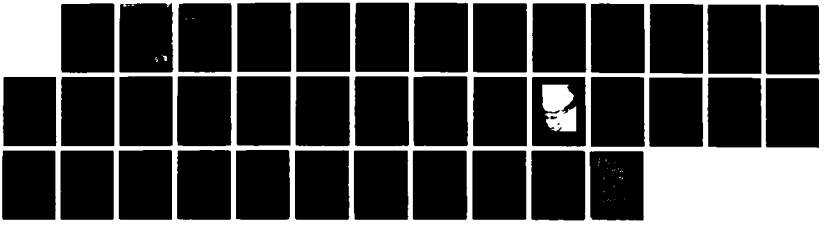

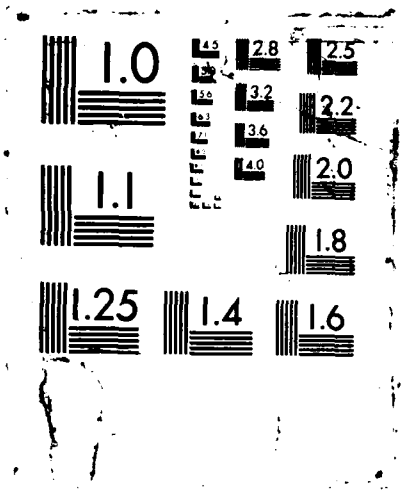
1.0
1.1
1.25
1.4
1.6
1.8
2.0
2.2
2.5
2.8
3.2
3.6
4.0

AFGL-TR-88-0020

On the Dynamics of the Auroral Ionosphere During the Breakup of a Substorm

Michael B. Silevitch

Northeastern University
Boston, MA 02115

1 March 1988

Final Report
January 28, 1983 - August 31, 1986

AIR FORCE GEOPHYSICS LABORATORY
AIR FORCE SYSTEMS COMMAND
UNITED STATES AIR FORCE
HANSCOM AIR FORCE BASE, MASSACHUSETTS 01731-5000

" This technical report has been reviewed and is approved for publication"

PAUL L. ROTHWELL
Contract Manager

NELSON C. MAYNARD
Branch Chief

FOR THE COMMANDER

RITA C. SAGALYN
Division Director

This report has been reviewed by the ESD Public Affairs Office (PA) and is releasable to the National Technical Information Service (NTIS).

Qualified requestors may obtain additional copies from the Defense Technical Information Center. All others should apply to the National Technical Information Service.

If your address has changed, or if you wish to be removed from the mailing list, or if the addressee is no longer employed by your organization, please notify AFGL/DAA, Hanscom AFB, MA 01731. This will assist us in maintaining a current mailing list.

Do not return copies of this report unless contractual obligations or notices on a specific document requires that it be returned.

UNCLASSIFIED
SECURITY CLASSIFICATION OF THIS PAGE A19225

REPORT DOCUMENTATION PAGE

1a. REPORT SECURITY CLASSIFICATION Unclassified	1b. RESTRICTIVE MARKINGS
2a. SECURITY CLASSIFICATION AUTHORITY	3. DISTRIBUTION / AVAILABILITY OF REPORT Approved for public release; Distribution unlimited
2b. DECLASSIFICATION / DOWNGRADING SCHEDULE	
4. PERFORMING ORGANIZATION REPORT NUMBER(S)	5. MONITORING ORGANIZATION REPORT NUMBER(S) AFGL-TR-88-0020
6a. NAME OF PERFORMING ORGANIZATION Northeastern University 6b. OFFICE SYMBOL (If applicable)	7a. NAME OF MONITORING ORGANIZATION Air Force Geophysics Laboratory
6c. ADDRESS (City, State, and ZIP Code) Boston, Massachusetts 02115	7b. ADDRESS (City, State, and ZIP Code) Hanscom AFB Massachusetts 01731-5000
8a. NAME OF FUNDING / SPONSORING ORGANIZATION 8b. OFFICE SYMBOL (If applicable)	9. PROCUREMENT INSTRUMENT IDENTIFICATION NUMBER F19628-83-K-0014
8c. ADDRESS (City, State, and ZIP Code)	10. SOURCE OF FUNDING NUMBERS

PROGRAM ELEMENT NO	PROJECT NO.	TASK NO	WORK UNIT ACCESSION NO
61102F	2311	G2	FC

11. TITLE (Include Security Classification)
On the Dynamics of the Auroral Ionosphere During the Breakup of a Substorm

12. PERSONAL AUTHOR(S)
Michael B. Silevitch

13a. TYPE OF REPORT	13b. TIME COVERED	14. DATE OF REPORT (Year, Month, Day)	15. PAGE COUNT
Final Report	FROM 1.28.83 TO 8.31.86	1988/03/01	38

16. SUPPLEMENTARY NOTATION

17 COSATI CODES			18. SUBJECT TERMS (Continue on reverse if necessary and identify by block number)
FIELD	GROUP	SUB-GROUP	Substorm evolution, Pi2 Pulsations

19. ABSTRACT (Continue on reverse if necessary and identify by block number)

The research investigation described here concentrated on several dynamic features of substorm evolution during its breakup phase. More specifically, we focussed upon the development of a model for the propagation of the Westward Travelling Surge (WTS) as seen from the viewpoint of an active ionosphere. We also considered a mechanism for the generation of Pi2 pulsations. An important feature of our approach is the natural coupling which exists between the WTS motion and the frequency spectrum of the Pi2 modes. Thus, our theory predicts the correlation of Pi2 waveforms to substorm onsets. This correlation seems to be a reasonable one in light of recent observations of substorm morphology.

20. DISTRIBUTION / AVAILABILITY OF ABSTRACT ☐ UNCLASSIFIED/UNLIMITED ☐ SAME AS RPT ☐ DTIC USERS	21. ABSTRACT SECURITY CLASSIFICATION Unclassified
22a. NAME OF RESPONSIBLE INDIVIDUAL Paul L. Rothwell	22b. TELEPHONE (Include Area Code) 22c. OFFICE SYMBOL AFGL/PHG

DD FORM 1473, 84 MAR 83 APR edition may be used until exhausted. All other editions are obsolete

SECURITY CLASSIFICATION OF THIS PAGE
UNCLASSIFIED

TABLE OF CONTENTS

--

I. INTRODUCTION

The research described in this report is one of the first attempts to construct a model for the temporal propagation of conductivity enhancements associated with the auroral ionosphere during substorm breakup. To place the research into a proper perspective we shall, in Section III, first review some of the observational facts relating to substorm morphology. Following that, we shall discuss our results and their relation to observations.

II. DESCRIPTION OF RESEARCH

The substorm phenomenon is a global process exhibiting complex dynamical features. It intrinsically involves the interaction of coupling between the solar wind, magnetosphere, and ionosphere. Phenomenoligically, the evolution of most substorms can be broken down into a series of distinct phases. Akasofu (1977) has schematically characterized the growth and decay of auroral substorm as shown in Figure II.1. The time between T=0 and 5 minutes denotes the onset

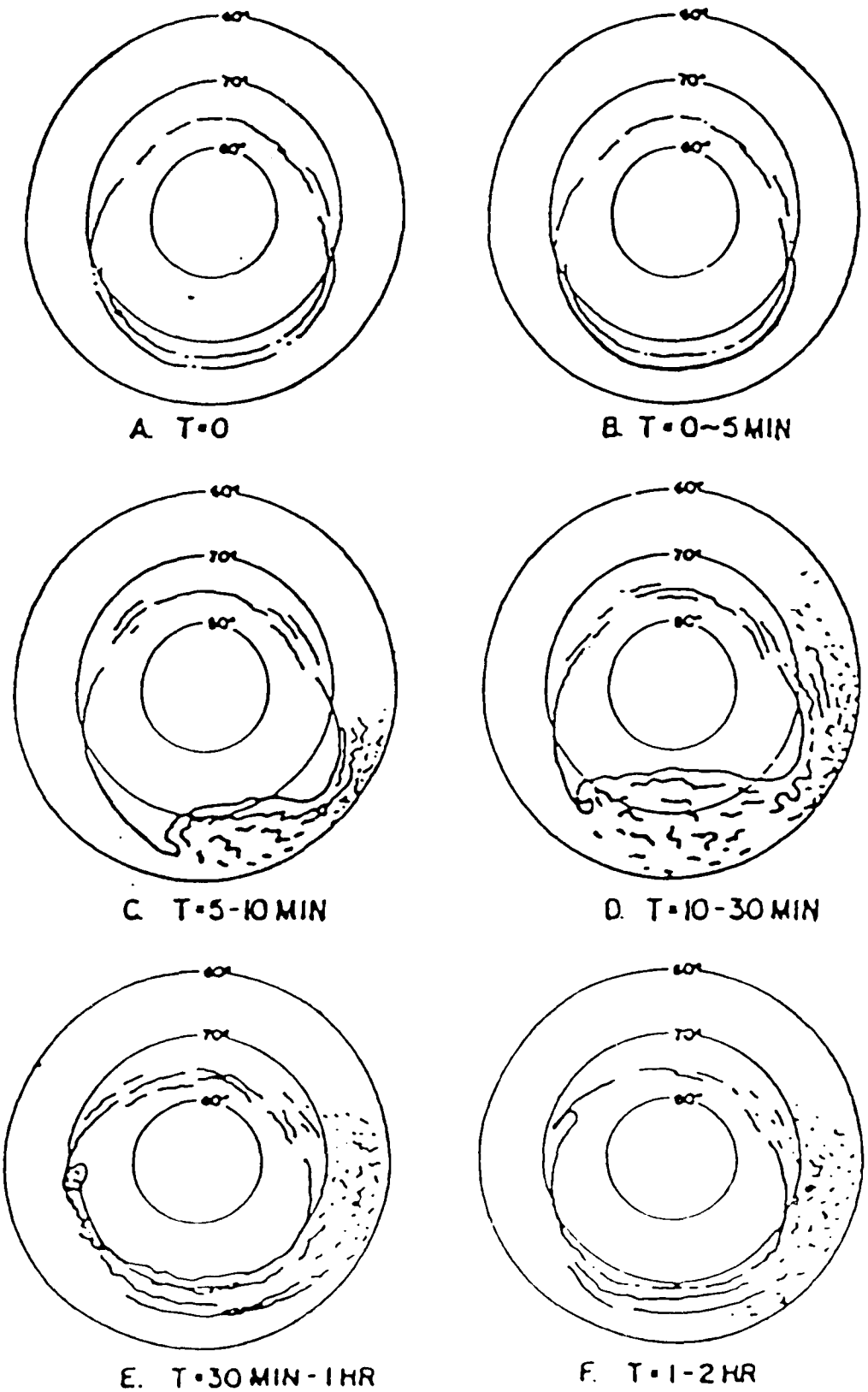

Fig. II.1 Schematic diagram showing the growth and decay of the auroral substorm, viewed from above.

of a substorm. It is characterized by an initial brightening and poleward expansion of a quite auroral arc (typically the most equatorward form). Indeed, this poleward motion of the auroral arc is often described as a "poleward leap" since the process has been observed to occur with speeds of 1 to 10 km/sec. Associated with the substorm is the generation of Pi2 pulsations. Following the initial or growth phase of the substorm, the phenomenon evolves in the manner shown in Figure 1C and 1D. This complex "breakup" phase of the substorm is characterized by the formation of a feature called the Westward Travelling Surge (WTS). As shown in Figure II.1, within 30 minutes after onset the auroral structure exhibits a twisting and simultaneous propagation towards the west. We shall discuss the properties of the WTS in more detail below when we describe our efforts to model the phenomenon. Following the breakup phase, the substorm enters its final or "recovery phase" wherein the auroral system moves back toward a configuration characteristic of quiescent conditions.

We can now use the brief "definition" of the substorm given above to put our research into a coherent framework. It was only within the last several years that systematic morphological properites were associated with WTS. Several important characteristic features of the surge are:

a) The structures can propagate in the ionosphere at speeds of 1 to 30 km/sec (Opgenoorth et al., 1983: Yahnin et al., 1983; G. Rostoker, private communication.). Indeed, these speeds are typically an order of magnitude higher than E x B drift velocities and are moreover often in the opposite direction. The instantaneous speeds of 30

km/sec have been observed in the leading branch of the westward electrojet. This "horn region" is westward of the WTS fold of Figure 1C.

b) The propagation of the WTS moves in steps rather than continuously (Wiens and Rostoker, 1975; Pytte et al., 1976).

c) Correlated with the WTS is the appearance of energetic precipitating electrons (typically 1 to 10 Kev). These fluxes pervade the high conductivity region associated with the surge (Meng et al., 1978).

d) At the end of the surge there exists an intense upward field aligned current carried by energetic precipitating electrons. This current is concentrated within an area of roughly 100 km x 100 km with an average intensity of 1-10 μAmp/m^2. This feature can be modeled as a line current carrying approximately 10^5 Amps (Inhester et al., 1981). It should be noted that the head of the surge corresponds to the fold that develops in Figure 1C and propagates as shown in Figures 1D and 1E.

e) There is clearly an observed relationship between the WTS and the generation of Pi2 pulsations during substorm onsets (Rostoker and Samson, 1981; Samson and Rostoker, 1984).

The foundation for research proposed here is contained in two papers which describe a model for the propagation of the WTS and the associated generation of Pi2 pulsations. These works are included herein as Appendices A and B. Both are the results of a collaboration between myself, P. Rothwell and L. Block. For reference we will denote as Paper 1 the work in Appendix A entitled, "A Model for the Propagation of the Westward Travellling Surge" (JGR 89, A10, 8941, Oct. 1984). Paper 2, entitled "Pi2 Pulsations and Westward Travelling Surge" (Appendix B), has been accepted for publication in JRGR. In describing our previous research we will concentrate upon summarizing the major results and refer to the appendices for the mathematical details.

II.1 Propagation of the Westward Travelling Surge

Steady state models of the WTS have been developed using preliminary ground-based observations (Hughes and Rostoker, 1979; Rostoker and Hughes, 1979; Tighe and Rostoker, 1981). A comprehensive static model of the electrodynamic structure within the WTS was developed by Inhester et al., (1981). This model is described in detail in Section 2 of Paper 1. Essentially, one can model the WTS at a given instant of time as a Cowling conductivity channel in the ionosphere. The channel is described as a slab aligned in the "east-west" direction. Examination of Figure II.1 above indicates that the slab approximation is a reasonable one for certain aspects of the complex WTS phenomenon (see eg., Figure 1B and horn region of Figures 1C and 1D). Modeling the surge head of Figures 1C, D and E by a slab is clearly only a first approximation. An improvement of this model is one of the research thrusts proposed here.

Kan et al., (1984) have pointed out the importance of the degree of ionospheric current closure on the poleward boundry of the enhanced conductivity region associated with the WTS. Closure is governed by the parameter α, which is a measure of th degree to which the net ionospheric current is continued into the magnetosphere via field aligned currents at the slab boundries (see Section 2 of Paper 1 for more details). In our context strong current closure ($\alpha = 1$) implies full continuation of the ionospheric current into the magnetosphere.

In Paper 1 we develop a dynamic model for the propagation of the WTS. We explicitly utilize the closure concept and incorporate it with elements of the Inhester-Baumjohann slab model (Baumjohann, 1983). The motion of the WTS in the midnight sector is considered to be controlled by three mechanisms. These are:

1) the energy and intensity of the precipitating electrons;

2) the electron-ion recombination rate;

3) the degree of current closure on the boundaries of the slab.

Both the closure parameter α and electron precipitation energy represent the magnetospheric input into the surge dynamics. At present these inputs are not self-consistently incorporated into our models. A consideration of this issue will be one of the important tasks in our proposed research program.

The main idea of Paper 1 can be expressed as follows (L. Block, private communiation, 1985). If a Birkeland current moves (e.g., due to some magnetospheric action) the connecting ionospheric current may encounter some relatively low conductivity regions. This could demand a higher voltage from the magnetospheric generator, unless the high conductivity region is able to follow the motion of the Birkeland current. The field aligned Birkeland current is itself an ionizing mechanism through the associated energetic electron precipitation especially in the upward current region. Hence, as the upward current moves it can give rise to a synchronous motion of the conductivity channel provided it doesn't move to rapidly. One can derive some relations between the Birkeland current intensity and the speed at which its footprint

moves in the ionosphere. The validity of this approach depends upon the assumption that one can obtain some relation between the field aligned current density and the ionizing efficiency of the associated precipitating electrons. This was in fact done in Paper 1 and a wave equation was derived. The velocity of propagation is proportional to $V_d QH$, where V_d is the magnitude of the total E x B drift velocity and QH is the height integrated ionization efficiecy for precipitating electrons at the conductivity gradient. It is a characteristic of QH that the velocity is greatly enhanced when the average precipitating electron energy increases from 1 Kev to 10 Kev. The variations of QH with energy are shown in Table 1 and Figure 3 of Paper 1. As an example we note that a 10 mV/m ionospheric electric field implies a propagation velocity of roughly 3.7 km/sec for 1 KeV incident electrons with 10 Kev electrons will produce a velocity of 34 km/sec. Thus, in applying this propagation mechanism to our slab model of the WTS we predict that jumps in the surge velocity will occur whenever there is a hardening of the energy spectrum of the precipitating electrons associated with the upward field aligned current region of the WTS.

The simple dynamical slab model of Paper 1 predicts a wide range of complex phenomena associated with the poleward leap, WTS propagation and recovery phase of a substorm. In this model the important parameters are the ratio of Hall to Pedersen conductivities, the degree of ionospheric current closure into the magnetosphere, and the energy spectra of the precipitating electrons. We will conclude this subsection by summarizing the major results of Paper 1. These are:

1) The direction of the WTS depends strongly on the degree of current closure on the poleward boundary. The sensitivity of the surge direction to closure depends on the ratio (R) of the Hall to the Pedersen conductivities.

2) The magnitude of the surve velocity is sensitive to the energy spectrum of the precipitating electrons and weakly dependent on R. The ratio of the surge velocity to the measured drift velocity is independent of the degree of closure at both the surge head and the northern boundary.

3 The initation of the expanse phase of the substorm can be explained by assuming that the initial arc brightening arises from a sudden hardening of the precipitating electron energy spectrum as its poleward boundary.

4) Inclusion of electron-ion recombination effects highlights the role of the precipitating current intensity in modulating the surge propagation and explains the equatorward retreat of the surge during the substorm recovery phase.

5) Details of the surge propagation depend on how the magnetosphere and ionosphere are coupled as reflected by the quantities α and Q. Hence the energy source is clearly located in the magnetosphere and a complete description of substorm phenomena must take this into account.

II.2 Generation of Pi2 Pulsations

The second major component of our previous research concerns an investigation into the generation of Pi2 pulsations and their correlation with substorm dynamics. As indicated above, the results of this work are detailed in Paper 2 which is reproduced here as Appendix B. As in the previous subsection we shall simply summarize the important results of this research and refer the reader to Paper 2 for specific derivations. To put our results into a coherent framework we first list three important characteristics in the Pi2 waveforms. These are:

a) The appearance of Pi2 wavetrains is correlated with the onset of a substorm.

b) The Pi2 waveform has a damped quasi-sinusoidal shape. The periods of the pulsations fall between 40 and 140 seconds. Their duration is typically on the order of several minutes. Figure 4 of Paper 2 shows some representative data for the Pi2 pulsations.

c) The polarization sense of the waveform changes if one compares observations inside and outside the regions of enhanced conductivity characteristic of substorm activity.

Paper 2 refines the dynamics of the simple slab model developed previously. To incorporate the generation of Pi2 waves we assume that the ionosphere-magnetosphere coupling can be modeled by a transmission line. This approach was

first developed by Sato (1978) and takes into account the propagation of transverse Alfven waves generated by perturbations that originate either in the ionosphere or magnetosphere. In our calculation we consider the effects of an ionospheric perturbation which occurs in the properties of the Cowling channel used to model the WTS dynamic. The effect of the transmission line coupling is to include the possibility of a feedback instability which can cause ionospheric disturbances to be amplified. This instability mechanism was first introduced by Atkinson (1970) and later refined by Sato and his co-workers. All previous work, however, had been applied to the properties of quiet auroralforms. To the best of our knowledge, Paper 2 represents the first attempt to utilize the feedback instability mechanism in a theory of substorm dynamics. The major results of Paper 2 are:

1) The use of the feedback instability coupled with the dynamical results of Paper 1 yields a theory which ties the generation of Pi2 pulsations of substorm onsets. In particular we have developed a perturbation scheme based on a closed set of nonlinear partial differential equations. To zeroth order our theory is exactly that of the bulk propagation of the WTS described in Paper 1. To first order we obtain a dispersion relation which reflects the feeback instability mechanism. The frequency and growth rate of the modes are shown in Figure 3 of Paper 2. There it is seen that the frequency range is characteristic of the Pi2 pulsation.

2) The frequency and growth (or damping) of the Pi2 waves is a function of WTS velocity. From Paper 1 this implies that the properties of Pi2s depend on the characteristics of the precipitating electrons associated with an enhanced conductivity region.

3) In Paper 1 it is found that the slab propagates only if the field aligned current exceeds a critical threshold wherein ionization dominates over recombination effects. For parameters characterizing substorm conditions the critical current value is on the order or $5\mu Amp/m^2$. When the current threshold is superimposed on the wave characteristics of Paper 2 it is found that the Pi2 modes are damped in agreement with physical constraints. This result will be discussed in more detail in Section IV.2.

REFERENCES

Akasofu, S.I., Physics of magnetospheric substorms, D. Reidel Publ., Co., Chap. 1; 1977.

Atkinson, G., Auroral arcs: result of the interaction of a dynamic magnetosphere with the ionosphere, J. Geophys. Res., 75, 4746-4754, 1970.

Baumjohann, W., Ionospheric and field-aligned current systems for in the auroral zone: a concise review, Adv. Space Res., 2, 55-62, 1983.

Fridman, M., and J. Lemaire, Relationships between auroral electron fluxes and field-aligned electric potential differences. J. Geophys. Res., 85, 664-670, 1980.

Hughes, T. J., and G. Rostoker, A comprehensive model current system for high-latitude magnetic activity. I, The steady-state system, Geophys. J. Astron. Soc., 58, 525-569, 1979.

Inhester, B., W. Baumjohann, R. A. Greenwald, and E. Neilson, Joint two-dimensional observations of ground magnetic and ionospheric electric fields associated with auroral zone currents, 3. Auroral zone associated during the passage of a westward traveling surges, J. Geophys., 49, 155-162,, 1981.

Kan, J. R., R. L. Williams, S. I. Akasofu, A mechanism for the westward traveling surges, J. Geophys., 89, 2211-2216, 1984.

Lysak, Robert L., Coupling of the dynamic ionosphere to auroral flux tubes, Accepted for publication, J. Geophys. Res, 1986.

Marklund, G. T., M. Raadu and P. A. Lindquist, Effects of birkland current limitation on high latitude convection patterns, J. Geophys. Res., 90, 10,864-10,875, 1985.

Meng, C. I., A. L. Snyder, Jr. and H. W. Kroehl, Observations of auroral westward traveling surges and electron precipitations, J. Geophys. Res., 83, 575-585, 1978.

Opgenoorth, H. J., R. J. Pellinen, W. Baumjohann, E. Nielsen, G. Marklund, and L. Eliasson. Three-dimensional current flow and particle precipitation in a westward traveling surge (observed during the Barium-GEOS rocket experiment), J. Geophys. Res., 88, 3138-3152, 1983.

Pytte, T., R.L. McPherron, and S. Kokubun, The ground signatures of the expansion phase during multiple onset substorms, Planet, Space Sci., 24, 1115-1132, 1976.

Rostoker, G., J. C. Samson, Polarization characteristics of Pi^2 pulsations and implications for their source mechanisms: location of source regions with respect to the auroral electrojets, Planet. Space Sci., 29, 225-247, 1981.

Sato, T., A theory of quiet aurorol arcs, J. Geophys. Res., 83, 1042-1048, 1978.

Singer, H.J., W. Jeffrey Hughes, Paul F. Fougere and David J. Knecht, The localization of Pi^2 pulsations: ground-satellite observations, J. Geophys. Res., 88, 7029-7036, 1983.

Southwood, D. J., and W. J. Hughes, Theory of hydromagnetic waves in the magnetosphere, Space Sci. Rev., 35, 301, 1983.

Tighe, W. G., and G. Rostoker, Characteristics of westward traveling surges during magnetic substorms, J. Geophys. Res., 50, 51-67, 1981.

Wiens, R.G., and G. Rostoker, Characteristics of the development of the westward electrojet during the expansive phase of magnetiospheric substorms, J. Geophys. Res., 80 2109-2128, 1975.

Yahnin, A. G., V. A. Sergeev, R. J. Pelinen, W. Baumjohann, K. A. Kalia, H. Ranta, J. Kangas, and O. M. Raspopov, Substorm time sequence and microstructure of 11 November 1976, J. Geophys., 53, 182-197, 1983.

APPENDIX A

JOURNAL OF GEOPHYSICAL RESEARCH, VOL. 89, NO. A10, PAGES 8941-8948, OCTOBER 1, 1984

A Model for the Propagation of the Westward Traveling Surge

PAUL L. ROTHWELL

Air Force Geophysics Laboratory, Bedford, Massachusetts

MICHAEL B. SILEVITCH

Department of Electrical Engineering, Northeastern University, Boston, Massachusetts

LARS P. BLOCK

Department of Plasma Physics, Royal Institute of Technology, Stockholm, Sweden

A unified model is developed for the propagation of the westward traveling surge (WTS) that can explain the diversity in the observed surge characteristics. We start with the Inhester-Baumjohann model for the surge region, which implicitly includes both the Hall and Pedersen currents. It is found that precipitating electrons at the conductivity gradient modify the gradient, causing it to propagate as a wave front. The velocity of propagation is directly dependent on the ionization efficiency of the precipitating electrons and therefore increases dramatically when they become more energetic during substorm onsets. For example, we predict that when the incident electron energy changes from 1 keV to 10 keV the surge velocity should increase from 2 km/s to 34 km/s. The direction of the surge motion depends on the presence of polarization charges on the poleward surge boundary. This is related to the efficiency with which the poleward ionospheric currents are closed off into the magnetosphere by the field-aligned currents. Inclusion of the electron-ion recombination rate modifies the surge propagation velocity and leads to explicit expressions for the conductivity profile. Sufficient precipitation current is required to overcome electron-ion recombination in order for the surge to expand. When the precipitating current is less than this threshold the WTS retreats. Therefore, the model describes the ionospheric response to both the expansion and recovery phases of the magnetic substorm.

1. INTRODUCTION

The westward traveling surge (WTS) is a primary signature of substorm onsets [*Rostoker et al.*, 1980]. In simplest terms the WTS represents the westward electrojet as it expands westward starting near local midnight during the substorm expansion phase [*Tighe and Rostoker*, 1981]. Figure 1 shows a typical WTS profile as measured by the DMSP satellite F-6. In this example we see evidence for multiple surge structure as described by *Rostoker et al.* [1980]. Note that the shape of the WTS is similar to that of oceans waves where the wave crest corresponds to a surge head. A more detailed examination of the surge reveals several characteristic features of the phenomena. These include the following: (1) The surge moves in discrete jumps or steps [*Wien and Rostoker*, 1975; *Pytte et al.*, 1976]. (2) Instantaneous velocities of up to 30 km/s have been observed in the leading branch of the westward electrojet [*Opgenoorth et al.*, 1983; *Yahnin et al.*, 1983, G. Rostoker, private communication, 1983). However, a typical surge velocity is on the order of 1.0-2.0 km/s [*Pytte et al.*, 1976]. (3) The energy of the precipitating electron flux associated with the surge region is usually in the keV range [*Meng et al.*, 1978]. (4) At the head of the surge there exists an intense upward field-aligned current carried by energetic precipitating electrons. This current is concentrated within an area of at least 100 km × 100 km (1° × 1°) with an average intensity of 1-10 $\mu A/m^2$ and can be modeled as a line current carrying $\cong 10^5$ A [*Inhester et al.*, 1981]. The slab model developed in section 2 can be applied to both the surge head and to the western precursor region.

Steady-state models of the WTS have been developed by *Hughes and Rostoker* [1979], *Rostoker and Hughes* [1979], and *Tighe and Rostoker* [1981] using primarily ground-based observations. By incorporating STARE data, *Inhester et al.* [1981] have developed a comprehensive static model of the electrodynamic structure within the surge. *Kan et al.* [1984] have pointed out the importance of ionospheric current closure on the poleward surge boundary. Using static conductivity models they show that closure is responsible for the westward intrusion of highly conductive regions. In the present dynamical model we explicitly show how closure determines the surge direction and, in contrast to their conclusions, find that the surge speed does not necessarily depend on the time rate of change of closure.

In this paper we develop a dynamic model for the propagation of the WTS. As shown in the next section we explicitly utilize the closure concept and incorporate it with elements of the Inhester Baumjohann model [*Baumjohann*, 1983]. The motion of the WTS in the midnight sector is considered to be controlled by three mechanisms. These are (1) the energy and intensity of the precipitating electrons, (2) the electron ion recombination rate, and (3) the degree of current closure on the poleward boundary of the surge. Closure is governed by the parameter α, which is a measure of the degree to which the net ionospheric current is continued into the magnetosphere at the poleward boundary (see discussion near equation (2) for more details). In our context, strong current closure ($\alpha = 1$) implies full continuation of the ionospheric Hall current system into the magnetosphere via field-aligned currents. Both α and the precipitation energy represent the magnetospheric input to the surge dynamics. The mechanisms describing these parameters are outside the scope of the present paper.

Upward field-aligned currents in the WTS are most intense where the conductivity gradient is largest. These currents are

Paper number 4A0864.

carried by precipitating electrons that modify the conductivity gradient through enhanced ionization. A wave equation is derived for the propagation of the conductivity gradient. The phase velocity is proportional to $V_{dt}QH$ where V_{dt} is the magnitude of the total $E \times B$ drift velocity and QH is the height-integrated ionization efficiency for precipitating electrons at the conductivity gradient. This velocity is greatly enhanced when the average electron energy increases from 1 keV to 10 keV. For example, a 10 mV/m electric field implies a surge velocity of approximately 3.7 km/s for 1-keV incident electrons, whereas 10-keV incident electrons will drive the surge at approximately 34 km/s (see Table 1 for details). We see no direct connection between this propagation mechanism and that based upon an ion-acoustic wave as proposed by *Kan et al.* [1984].

The effect is to produce jumps in the surge velocity whenever the precipitating energy spectrum near the surge head is sufficiently hard. As shown below, it is even possible to have abrupt northeastward surge motion if there is overclosure at the poleward boundary (i.e., $\alpha > 1$). Thus even this simplified model provides coherence to the diversity of observed surge propagation characteristics.

In section 2 the simplified model is developed for the WTS where electron ion recombination effects are ignored. The magnitude of the surge velocity and its direction are derived. In section 3 we investigate the role of electron-ion recombination effects. We find that the recombination rate modifies the surge velocity, determines the conductivity profile at the boundary, and is responsible for the retreat of the enhanced conductivity region and the associated electrojet during the recovery phase.

2. A Model for the Westward Traveling Surge

We start with the slab model for the WTS near local midnight as given by *Baumjohann* [1983] and as shown in Figure 2. In this section we only consider the motion of this slab. The results will be applied to the WTS in the discussion section. For clarity the stated propagation directions are defined for the WTS occurring in the northern hemisphere. An effective westward electric field, E_0, in the surge region drives a northward Hall current. This electric field is composed of the large-scale convection field and that produced by negative charge

current is

$$J_H = \Sigma_H E_0 \tag{1}$$

However, the net ionospheric current reaching the northern boundary may be unequal to J_H depending on the presence of boundary polarization charges as indicated in Figure 2. This boundary polarization charge produces a southward polarization electric field, E_p, as shown in the figure. This electric field gives rise to an associated Pedersen current, $J_p = \Sigma_p E_p$. Thus, the net ionospheric current reaching the northern boundary is $J_n = J_H - J_p = \Sigma_H E_0 - \Sigma_p E_p = \alpha J_H$, where the parameter α is a measure of the polarization charge at the slab boundaries. It is also a measure of the degree to which the net ionospheric current is closed into the magnetosphere by field-aligned currents (assuming no ionospheric current closure outside the region). It is an undetermined parameter in our theory that requires [illegible] ionosphere magnetosphere coupling. The value $\alpha = 0$ is for full closure, the value $\alpha = 1$ full closure and $\alpha > 1$ overclosure (i.e., a negative polarization charge on the northern boundary produced by excess Birkeland currents).

We define a coordinate system as shown in Figure 2 such that the z axis points perpendicular to both the current channel and the earth's magnetic field. The x axis points parallel to the current channel. When applied to the westward electrojet the x coordinate is approximately west and the z coordinate north. For simplicity, in the following model we define x as pointing due west and z as pointing due north.

The precipitating Birkeland current is the divergence of J_n as given by

$$j_\parallel = -\partial(E_0 \alpha \Sigma_H)/\partial z$$
$$= -E_0 \alpha \partial \Sigma_H / \partial z \tag{2a}$$

where α is the coupling parameter defined above. A meaningful α can only be defined where there is a conductivity gradient. To be more precise, consider current conservation across the boundary.

$$\int_{z_1}^{z_2} j_\parallel \, dz = \int_{z_1}^{z_2} -E_0 \partial(\alpha(z)\Sigma_H(z)) \, dz \tag{2b}$$

If α = const. within the boundary region ($z_1 \le z \le z_2$), then

$$\int_{z_1}^{z_2} j_\parallel \, dz = \alpha J_H(z_1) \tag{2c}$$

This is another way of expressing the overall current continuity at the northern boundary. An $\alpha < 1$ implies the presence of positive polarization charge. We associate $j_\parallel$ with the flux of precipitating electrons through the relation $j_\parallel/e$. This assumes that the precipitating protons are not important in the surge region [*Akasofu et al.*, 1969] and that the dominant current carriers are energetic (keV) electrons [*Meng et al.*, 1978; *Inhester et al.*, 1981]. This is consistent with the observed enhancement of keV electrons observed during the passage of the WTS [*Opgenoorth et al.*, 1983]. For simplicity we shall ignore possible spatial variations in both α and E_0. The ratio of the Hall to Pedersen conductivity (R) is considered to be a function of z only.

In the following derivation we recognize that precipitating electrons through ionization modify the conductivity. The electron flux, $j_\parallel/e$, may consist of electrons that are accelerated at higher altitudes through field-aligned potential differences. In that case $j_\parallel/e$ is the flux of accelerated electrons incident on the ionosphere. The local time rate of change of the Hall conductivity is

$$\partial \Sigma_H / \partial t \simeq (eH/B)\partial n / \partial t \tag{3}$$

where n is the ion density that is related to the precipitating electrons through the ionization efficiency Q [*Rees*, 1963; *Jasperse and Basu*, 1982]. The local time rate of change of the ion number density is given by

$$\partial n / \partial t = Qj_e - \sigma_r n^2 \tag{4}$$

where here Q is the average number of ions produced per incident electron-m and H is the appropriate height interval for Q and σ_r is the electron ion recombination coefficient in the ionosphere. (The unit ions/electron-m when multiplied by the unit for flux (electron/m^2-s) becomes ions/m^3 s, the ion production rate per unit volume). Equation (4) is general in that an average Q can be defined for any incident spectrum. The ionization rate is then this average Q times the total incident electron current providing the net backscattered current is small. For example, the presence of a parallel electric

Fig. 1. The aurora as photographed by the DMSP-F6 satellite on January 17, 1983. A small westward traveling surge (WTS) is observed in the center of the photograph followed by a significantly larger one to the east. The overall shape of a surge is similar to that of an ocean wave where the wave crest corresponds to the surge head. In our idealized model the surge is represented as a slab as shown in Figure 2.

field will effectively eliminate any upward electron current contribution [*Evans*, 1974]. If we assume that only the energetic component (keV electrons) carry the parallel current then the Q in equation (4) is identical to the Q / defined by *Rees* [1963].

We initially treat the limiting case where $\alpha Q \epsilon \gg \sigma_r n^2$ in order to illustrate the physical principles involved. The full equation is solved below in section 3. There we show that the simple approximation is valid if $j_{\parallel} \gg 3\ \mu A/m^2$ when $E_{incid} > 1$ keV. The sign in front of $j_{\parallel}$ in (4) indicates that positive current is flowing away from the earth. Combining (2)–(4) we obtain

$$\partial \Sigma_H / \partial t = -(QHE_0\alpha)/B\partial \Sigma_H/\partial z \qquad (5)$$

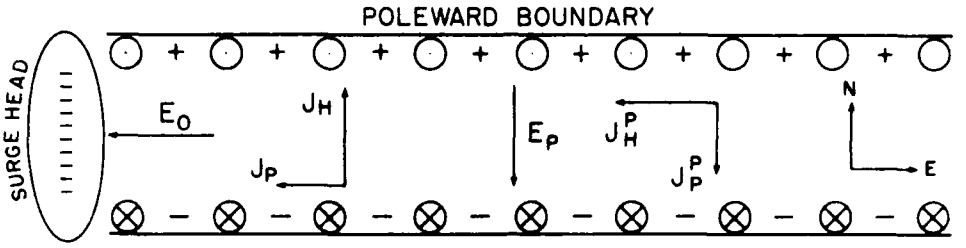

Fig. 2. Idealized model of the WTS as proposed by *Inhester et al.* [1981]. The total external electric field E_0 drives a westward Pedersen and a northward Hall current. If the northward Hall current is not fully continued by field-aligned currents into the magnetosphere polarization charges build up on the northern surge boundary producing a southward directed electric field E_p. This southward electric field produces a Hall current in the same direction as the Pedersen current from the original electric field E_0. This affects the direction of the surge motion as described in the text. Negative polarization charge may also build up at the surge head due to intense electron precipitation [*Inhester et al.*, 1981]. This is treated in our idealized model by allowing a renormalization of E_0. In our coordinate system, z points perpendicular to E_0 and x is parallel to E_0, which approximately corresponds to north and west.

which is a wave equation with a phase velocity given by

$$V_n = QH\alpha V_d \tag{6}$$

and where $V_d = E_0/B$. Note that (5) is also invariant under the Galilean transformation $\Sigma_H = \Sigma_H(z')$, where $z' = z - V_n t$.

Figure 3 shows the estimated variation of QH with incident electron energy as taken from Figure 2 of *Rees* [1963]. From this figure it is seen that a 1-keV monoenergetic precipitating flux implies $QH \simeq 10$ and for a 10 keV flux $QH \simeq 90$. Thus, when the energy spectrum of the precipitating electrons hardens the boundary velocity can increase by factors of 10. *Meng et al.* [1978] have measured a very hard precipitating energy spectrum in the surge region. We argue that the surge velocity is related to the production of energetic electrons connected with substorm onsets. According to this mechanism the surge velocity should increase dramatically during substorm onsets as has been observed by *Samson and Rostoker* [1983].

We now consider the western boundary (i.e., the surge head). The dynamics of this boundary is connected to the propagation of the poleward boundary through closure. That is, a small α implies a large E_p which drives a westward Hall current that adds to the Pedersen current driven by E_0. The total westward current is given by

$$J_w = \Sigma_p E_0 + \Sigma_H E_p \tag{7}$$

TABLE 1. Height Integrated Ion Production (QH) From Precipitating Electrons

keV	H, km	Q, ions/cm	QH, ions/cm	V_{to}, km/s ($\alpha = 1$, $R = 3.0$, $E = 15$ mV/m)
1	20	5×10^{-6}	10	3.7
5	10	8×10^{-7}	8	3.0
10	7	7×10^{-6}	49	18.7
100	5	8×10^{-4}	400	150.0

The height-integrated ion production (QH) from precipitating electrons is listed as a function of incident electron energy. These values were estimated from Figure 2 in the article by *Rees* [1963]. The appropriate height interval H is estimated at the maximum value of Q. The incident electrons are considered to be isotropic, monoenergetic beams. The results are plotted in Figure 3. The parameter α measures how efficiently the poleward Hall current closes into the magnetosphere. R is the ratio of the Hall and Pedersen conductivities, and E is the measured (see equation (15)) electric field in the ionosphere. V_{to} is the total surge velocity as defined in (14).

From the above definition of J_n we have

$$\begin{aligned} J_p &= (1 - \alpha)J_H \\ \Sigma_p E_p &= (1 - \alpha)\Sigma_H E_0 \end{aligned} \tag{8}$$

Substituting this expression for E_p into (7) leads to an α-dependent Cowling current

$$J_w = \{1 + R^2(1 - \alpha)\}E_0\Sigma_p \tag{9}$$

where

$$R = \Sigma_H/\Sigma_p$$

The precipitating current at the head of the surge is

$$\begin{aligned} j_{\parallel} &= \{1 + R^2(1 - \alpha)\}E_0\partial\Sigma_p/\partial x \\ j_{\parallel} &= [\{1 + R^2(1 - \alpha)\}E_0/R]\partial\Sigma_H/\partial x \end{aligned} \tag{10}$$

where the x axis is in the westward direction and R is considered independent of x. Note that at the northern boundary it was not necessary to assume R constant in deriving (5). Therefore, E_p (equation (8)) may also be a function of z, and our model implicitly allows polarization charge along the northern boundary. A wave equation is now derived for the western boundary associated with the surge head just as for the northern boundary. The resulting phase velocity is

$$V_w = QHV_d\{1 + R^2(1 - \alpha)\}/R \tag{11}$$

We now assume that the surge head region will propagate in a direction determined by the vector sum of V_n and V_w. The direction of the resultant surge velocity based on this idealized model is given by

$$\tan\gamma_s = V_n/V_w = \alpha R\{1 + R^2(1 - \alpha)\} \tag{12}$$

where $\gamma_s = 0$ corresponds to due west motion. We see that the direction of the surge is highly dependent on the degree of closure on the northern surge boundary and the value of R on the western surge boundary. For zero closure ($\alpha = 0$) the surge moves due west. For complete closure ($\alpha = 1$) the direction is almost due north [$\tan\gamma_s = R \cong 3$; $\gamma_s \simeq 72$].

The sensitivity of γ_s to α is modulated by the magnitude of R. A detailed plot of γ_s versus α for various values of R is shown in Figure 4. Note that the surge direction can range from due west to northeast, where the latter condition will arise when there is significant overclosure ($\alpha > 1$) during periods of intense electron precipitation.

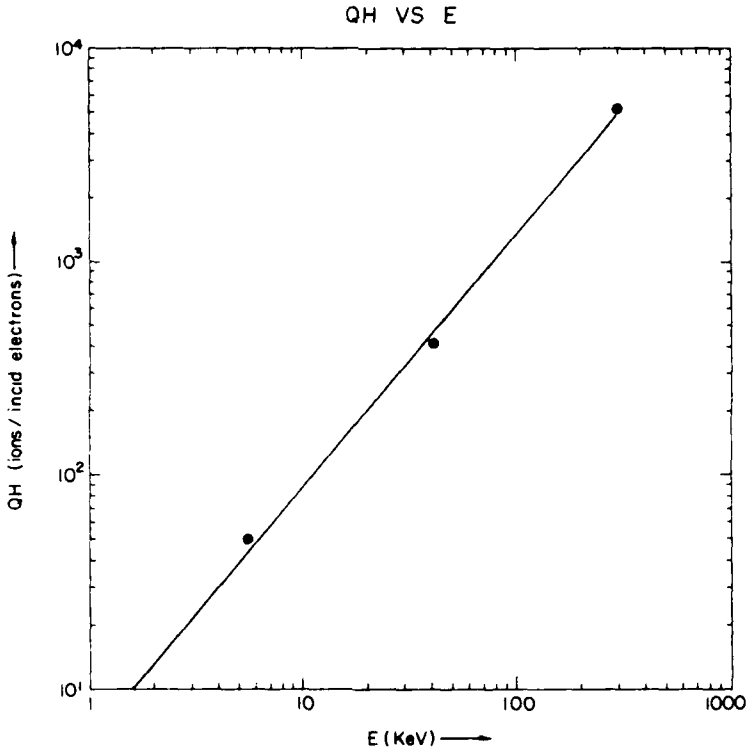

Fig. 3. Height-integrated ion production efficiency in the ionosphere for incident precipitating electrons. More energetic electrons produce a higher ionization density near the end of range. This curve is for an isotropic, monoenergetic incident beam and was taken from Figure 2 of *Rees* [1963]. Errors up to a factor of 2 could arise from erroneous estimation of the appropriate height interval from Rees' Figure 2. A reasonable fit to this curve is $QH \approx 5\ E^{1.2}$ ions/(incident electron).

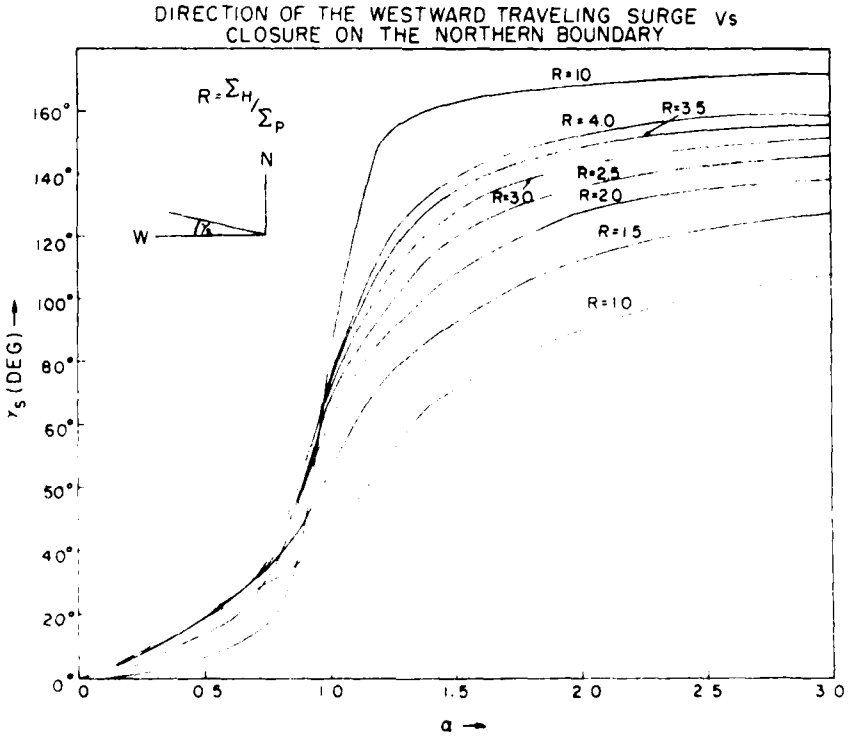

Fig. 4. The direction of the surge motion as a function of the closure parameter α, which represents the degree of Hall current closure on the northern surge boundary. The value $\alpha = 1$ implies $E_p = 0$. Also a larger value of α implies a more intense precipitating current with $\alpha > 1$ corresponding to a negative rather than positive charge buildup on the northern boundary. The sensitivity of the surge direction to α is dependent on the ratio of the Hall to Pedersen conductivities at the western surge boundary, which we denote by R. Note that $\gamma_s \simeq 45°$ corresponds to $\alpha \simeq 0.8$–0.9.

The magnitude of the total slab velocity, V_{ts}, is found from $V_{ts}^2 = V_n^2 + V_w^2$. Clearly, the resultant motion of the surge head is more complex than that indicated by the simple slab model treated here. (See discussion for more details.) Note that the slab velocity V_{ts} can be much larger the $E \times B$ speed and is in a different direction. From this definition of V_{ts} and equations (6) and (11) we find that

$$V_{ts} = V_d \frac{QH}{R} \{\alpha^2 R^2 + (1 + R^2(1 - \alpha))^2\}^{1/2} \quad (13)$$

Using the identity $\alpha^2 = (1 - \alpha)^2 - 1 + 2\alpha$ in V_{ts}, one finds (see appendix) that the total slab velocity can be expressed simply as

$$V_{ts} = V_{dt} QH\{1 + 1/R^2\}^{1/2} \quad (14)$$

which is independent of α and where V_{dt} is proportional to the total $E \times B$ speed as given by

$$V_{dt} = V_d\{E_0^2 + E_p^2\}^{1/2}/E_0 \quad (15)$$

Using (8) we have

$$V_{dt} = V_d\{1 + R^2(1 - \alpha)^2\}^{1/2} \quad (16)$$

It has been noted by *Opgenoorth et al.* [1983] that the measured electric field within and south of the auroral forms connected with the passage of a WTS was typically below the threshold (~15 mV m) of the STARE radar. This gives an upper limit to the drift velocity V_{dt} of 0.375 km/s. For V_{ts} (equation (14)) to equal the measured surge velocity of 2.0–3.3 km/s QH must be, therefore, on the order of 10. This implies from Figure 2 that the mean electron precipitation energy was on the order of 1 keV, which is consistent with observations [*Opgenoorth et al.*, 1983]. More comprehensive auroral campaigns are needed to simultaneously define the parameters used in our model.

3. Effects of Electron–Ion Recombination

In this section we include the effects of the electron–ion recombination rate on the WTS. One exact solution to (4) can be obtained by assuming an ionospheric magnetospheric coupling such that $\alpha = \Sigma_H^{-1}$ is a constant. The equation for Σ_H at the northern boundary is now

$$\partial\Sigma_H/\partial t = -V_n \partial\Sigma_H/\partial z - G\Sigma_H^2 \quad (17)$$

where

$$G = \sigma_r B/eH \quad (18)$$

and where V_n is defined in (6).

We now look for a solution to (17) that is stationary in a coordinate system (z') moving with a velocity V relative to the earth's surface. Accordingly, we make a Galilean transformation $z' = z - Vt$. This allows (17) to be rewritten as

$$\Sigma_H' - \Sigma_H^2 = G(V - V_n) \quad (19)$$

where $\Sigma_H' = \Sigma_H(z')$ and $\Sigma_H' = \partial\Sigma_H/\partial z'$. Note by definition that (19) is solely a function of z' in the moving frame of reference and, therefore, $\Sigma_H(z')$ is stationary in this frame. The solution is

$$\Sigma_H(z') = \Sigma_{Ho}(V - V_n)/(V - V_n - \Sigma_{Ho}Gz') \quad (20)$$

where $\Sigma_{Ho} = \Sigma_H(0)$. Hence, choosing α = constant implies that the conductivity profile is hyperbolic in the moving frame. We take $z' = 0$ to be where the boundary region joins the main ionosphere region in the Vaisberg–Iohester Baumjohann model. Therefore, Σ_{Ho} has the same value as the conductivity inside the surge head.

The assumed constant velocity V can now be expressed in terms of the conductivity gradient at $z' = 0$. To see this we first take the derivative of (20) and evaluate it at $z' = 0$. The resulting expression is

$$\Sigma_{Ho}' = G\Sigma_{Ho}^2/(V - V_n) \quad (21)$$

where Σ_{Ho}' is the value of the conductivity gradient at $z' = 0$. The physical meaning of (21) is made clearer by using equation (2) and solving for V. We find

$$V = V_n - G\Sigma_{Ho}^2 E_0 \alpha / j_\parallel(0) \quad (22)$$

We have previously shown that V_n increases dramatically as the incident energy spectrum hardens. The recombination term is independent of Q and, therefore, V also increases in the same manner.

Evidently, the slab boundary will not move poleward unless

$$j_\parallel(0) > G\Sigma_{Ho}^2 E_0 \alpha V_n = \sigma_r n^2 e^2 Q \quad (23)$$

Taking $\sigma_r \approx 10^{-13}$ m^3/s [*Walls and Dunn*, 1974], $n = 3 \times 10^{11}$ ions/m^3, and $Q = 5 \times 10^{-4}$ (electron-m)$^{-1}$ ($E_{in} = 1$ keV) we find a threshold current of 2.9 μA/m^2. This value is consistent with typical auroral current densities.

The precipitation current, therefore, must exceed some minimum value for the surge to propagate. Equation (22) also implies that if the current is below the threshold value the surge will propagate in a negative or equatorward direction. This, we believe, describes the ionospheric response during the recovery phase of a magnetic substorm. The diminishing precipitation current cannot sustain the high conductivity against electron–ion recombination and the surge head retreats.

Equation (17) can be solved at the western slab boundary in exactly the same way, except now V_n is replaced by V_w as defined in (11). The resulting effective velocity depends on the conductivity gradient at the western boundary. The conductivity gradients, therefore, must also influence the surge's direction of propagation as derived in section 2.

It should be emphasized that (17) could be solved because we assumed a specific ionospheric magnetospheric coupling such that a stationary solution was possible in a moving frame of reference. No doubt the dynamical nature of the coupling is such that the conductivity profile is probably nonstationary in all frames of reference. However, the present theory qualitatively explains much of the surge phenomena by using presently available data.

4. Discussion

It has been observed that the WTS moves in a series of discrete steps or jumps [*Wiens and Rostoker*, 1975; *Pytte et al.*, 1976]. This result led *Rostoker et al.* [1980] to define a magnetospheric substorm as allowing a series of multiple surges during the expansion phase. Each surge corresponds to an individual substorm onset that on a time average shifts the maximum poleward expansion northwestward. In the present model each surge corresponds to a temporal hardening of the precipitating electron flux energy spectrum. This temporal hardening is related to the substorm onset processes in the magnetotail and the generation of parallel electric fields which is outside the scope of the present work.

Samson and Rostoker [1983] noted the presence of associated Pi 2 signatures with the WTS. The surge marks the transition from equatorward to poleward type Pi 2 polarization signatures. The elliptical polarization of the Pi 2's is con-

sidered to be caused by the longitudinal expansion of field-aligned currents in the surge together with the conjugate reflection of field-aligned current pulses. We suggest that the same enhanced field-aligned current produces a jump in the surge velocity as predicted by the model presented here and as observed by *Wiens and Rostoker* [1975] and *Pytte et al.* [1976].

The surge head may at times break off from the main body forming a separate surge. (See Figure 13 in the paper by *Samson and Rostoker* [1983].) In terms of the present theory, once a new conductivity gradient is established between the surge regions their relative velocity is determined by the energy spectra of the precipitating electrons at the westward head of the separate parts. The propagation of each part can be described by modeling them as a separate slab. Instantaneous velocities of up to 30 km s have been observed at the leading branch of the western electrojet [*Opgenoorth et al.*, 1983; G. Rostoker, private communication, 1983]. This branch can be considered as a separate slab with its own model parameters. Westward velocities of 30 km s will result from (11) if we assume $E_0 = 10^{-2}$ V m, $\alpha = 0$, $R = 3$, and the incident electron energy to be approximately 5 keV. The higher westward velocities at the same precipitation energy are due to the additional R factor in V_w, which arises from the enhanced Cowling current when $\alpha = 0$. *Yahnin et al.* [1983] note that a harder precipitation energy exists inside the surge in comparison with outside the surge region which is consistent with this result.

Surges have also been occasionally observed moving in a northeasterly direction [*Pytte et al.*, 1976]. This can be explained in the present model by overclosure of the Hall current on the poleward surge boundary as shown in Figure 4. Intense electron precipitation ($\alpha > 1$) causes a poleward polarization electric field with an associated eastward Hall current that weakens the westward Pedersen current driven by the external electric field E_0.

The direction of the surge motion is related to the direction of the resultant electric field. From Figure 4 it is noted that a northwestward direction corresponds to $\alpha \simeq 0.8$–0.9. Using this result in (8) for E_p implies that the resultant electric field points in the southwestern direction that is consistent with the results of *Inhester et al.* [1981].

Our results in section 2 (summarized in Table 1 for $\alpha > 1$) indicated that an unphysical surge velocity could occur if the incident energy spectrum is too hard. However, in section 3 we found that the surge velocity is decreased by the electron ion recombination rate and that the magnitude of the precipitating current is important. Note also that the relation between α and the incident energy spectrum is unknown so that the excessive velocities given in Table 1 probably do not occur.

In summary, it is found that the present model predicts a wide range of complex surge phenomena depending on the ratio of the Hall to Pedersen conductivities, the degree of ionospheric current closure into the magnetosphere and the energy spectra of precipitating electrons. The following summarizes our main results.

1. We find that the direction of the WTS depends strongly on the degree of current closure on the poleward boundary. The sensitivity of the surge direction to closure depends on the ratio (R) of the Hall to the Pedersen conductivities.

2. The magnitude of the surge velocity is sensitive to the energy spectrum of the precipitating electrons and weakly dependent on R. The ratio of the surge velocity to the measured drift velocity is independent of the degree of closure at both the surge head and the northern boundary.

3. The expansion phase of the substorm is explained by assuming that the initial arc brightening arises from a sudden hardening of the precipitating electron energy spectrum at its poleward boundary.

4. Inclusion of electron ion recombination effects highlights the role of the precipitating current intensity in modulating the surge propagation and explains the equatorward retreat of the surge during the substorm recovery phase.

5. Details of the surge propagation depend on how the magnetosphere and ionosphere are coupled as reflected in the functional form of α and Q. Hence the energy source is clearly located in the magnetosphere and a complete description of substorm phenomena must take this into account.

APPENDIX

Equation (14) is obtained from (13) by using the given identity. The intermediate results for the bracketed term in (13) are

$$\begin{aligned}(1-\alpha)^2R^2 + 1 + R^2 + R^4(1-\alpha)^2 &= (1-\alpha)^2R^2[1+R^2] + 1 + R^2 \\ &= (1+R^2)[1+(1-\alpha)^2R^2] \end{aligned} \tag{A1}$$

Comparison of this expression with (16) immediately gives (14).

Acknowledgments. We would like to acknowledge stimulating discussions and pertinent comments by G. Rostoker, C.-G. Falthammar, W. J. Burke, W. J. Hughes, H. Singer, and C. Gelpi. One of us (MBS) would like to acknowledge support under U.S. Air Force contract F19628-83-K-0014.

The Editor thanks W. Baumjohann and another referee for their assistance in evaluating this paper.

REFERENCES

Akasofu, S.-I., R. H. Eather, and J. N. Bradbury, The absence of the hydrogen emission (H_β) in the westward traveling surge, *Planet. Space Sci.*, *17*, 1409–1412, 1969.

Baumjohann, W., Ionospheric and field-aligned current systems in the auroral zone: A concise review, *Adv. Space Res.*, *2*, 55–62, 1983.

Evans, D. S., Precipitating electron fluxes formed by a magnetic field aligned potential difference, *J. Geophys. Res.*, *79*, 2853–2858, 1974.

Hughes, T. J., and G. Rostoker, A comprehensive model current system for high-latitude magnetic activity, 1, The steady-state system, *Geophys. J. Astron. Soc.*, *58*, 525–569, 1979.

Inhester, B., W. Baumjohann, R. A. Greenwald, and I. Nielsen, Joint two-dimensional observations of ground magnetic and ionospheric electric fields associated with auroral zone currents, 3, Auroral zone currents during the passage of a westward traveling surge, *J. Geophys.*, *49*, 155–162, 1981.

Jasperse, J. R., and B. Basu, Transport theoretic solutions for auroral proton and H atom fluxes and related quantities, *J. Geophys. Res.*, *87*, 811–822, 1982.

Kan, J. R., R. L. Williams, and S.-I. Akasofu, A mechanism for the westward traveling surge during substorms, *J. Geophys. Res.*, *89*, 2211–2216, 1984.

Meng, C.-I., A. L. Snyder, Jr., and H. W. Kroehl, Observations of auroral westward traveling surges and electron precipitations, *J. Geophys. Res.*, *83*, 575–585, 1978.

Opgenoorth, H. J., R. J. Pellinen, W. Baumjohann, E. Nielsen, G. Marklund, and I. Eliasson, Three-dimensional current flow and particle precipitation in a westward traveling surge (observed during the Barium-GEOS rocket experiment), *J. Geophys. Res.*, *88*, 3138–3152, 1983.

Pytte, T., R. L. McPherron, and S. Kokubun, The ground signatures of the expansion phase during multiple onset substorms, *Planet. Space Sci.*, *24*, 1115–1132, 1976.

Rees, M. H., Auroral ionization and excitation by incident energetic electrons, *Planet. Space Sci.*, *11*, 1209–1218, 1963.

Rostoker, G., and T. J. Hughes, A comprehensive model current

system for high-latitude magnetic activity, II, The substorm component, *Geophys. J. Astron. Soc.*, *58*, 571–581, 1979.

Rostoker, G., S.-I. Akasofu, J. Foster, R. A. Greenwald, Y. Kamide, K. Kawasaki, A. T. Y. Lui, R. L. McPherron, and C. T. Russell, Magnetospheric substorms: Definitions and signatures, *J. Geophys. Res.*, *85*, 1663–1668, 1980.

Samson, J. C., and G. Rostoker, Polarization characteristics of Pi 2 pulsations and implications for their source mechanisms: Influence of the westward traveling surge, *Planet. Space Sci.*, *4*, 435–458, 1983.

Tighe, W. G., and G. Rostoker, characteristics of westward traveling surges during magnetic substorms, *J. Geophys.*, *50*, 51–67, 1981.

Walls, F. L., and G. H. Dunn, Measurement of total cross-sections for electron recombination with NO^+ and O_2^+ using ion storage technology, *J. Geophys. Res.*, *79*, 1911–1915, 1974.

Wiens, R. G., and G. Rostoker, Characteristics of the development of the westward electrojet during the expansive phase of magnetospheric substorms, *J. Geophys. Res.*, *80*, 2109–2128, 1975.

Yahnin, A. G., V. A. Sergeev, R. J. Pellinen, W. Baumjohann, K. A. Kaila, H. Ranta, J. Kangas, and O. M. Raspopov, Substorm time sequence and microstructure on 11 November 1976, *J. Geophys.*, *53*, 182–197, 1983.

L. P. Block, Department of Plasma Physics, Royal Institute of Technology, Stockholm, Sweden S10044.

P. L. Rothwell, Air Force Geophysics Laboratory, Hanscom Air Force Base, Bedford, MA 01731.

M. B. Silevitch, Department of Electrical Engineering, Northeastern University, Boston, MA 02115.

(Received December 28, 1983;
revised June 11, 1984;
accepted June 12, 1984.)

APPENDIX B

JOURNAL OF GEOPHYSICAL RESEARCH, VOL. 91, NO. A6, PAGES 6921-6928, JUNE 1, 1986

Pi 2 Pulsations and the Westward Traveling Surge

PAUL L. ROTHWELL

Air Force Geophysics Laboratory, Hanscom Air Force Base, Massachusetts

MICHAEL B. SILEVITCH

Department of Electrical Engineering, Northeastern University, Boston, Massachusetts

LARS P. BLOCK

Department of Plasma Physics, Royal Institute of Technology, Stockholm

A model is developed that relates the poleward leaps of the westward traveling surge (WTS) and the generation of Pi 2 pulsations. The feedback instability developed by Sato and coworkers is combined with the dynamic surge model of Rothwell et al. (1984). We find that our previous results on the motion of the WTS are related to the zero-order terms in the Sato formulation. The linearized first-order terms give rise to a dispersion relation with solutions in the Pi 2 frequency range. The lth frequency, f_l, is found to be turned on in integer multiples of one-half the Alfvén bounce frequency between the ionosphere and the plasma sheet. Most important, however, is that the lth frequency is turned on only when the precipitating electron energy exceeds a certain value. As previously shown, the velocity of the poleward surge boundary also increases when the energy of the precipitating electrons is enhanced. Therefore the poleward leap of the surge during substorm onsets is accompanied by the generation of higher Pi 2 frequency components. The time evolution of the composite Pi 2 pulse is obtained using the calculated decay rates, and agreement with data is shown.

INTRODUCTION

A recent review of Pi 2 pulsations and substorm onsets has been given by *Baumjohann and Glassmeier* [1984]. On the basis of previous work by *Rostoker and Samson* [1981] and *Samson and Rostoker* [1983] there is clearly an observed relationship between the westward traveling surge (WTS) and the generation of Pi 2 pulsations during substorm onsets. In particular, the WTS marks the longitudinal transition from the equatorward to poleward Pi 2. A poleward Pi 2 exists within the surge head and to the east. An equatorward Pi 2 predominates equatorward and to the west of the surge [*Rostoker and Samson*, 1981]. The maximum intensities of the Pi 2 pulsations were found along the equatorward boundaries of the electrojets. This led *Rostoker and Samson* [1981] and *Samson and Rostoker* [1983] to suggest that the resonance region of the Pi 2 pulsations is localized within the surge region and is constrained to remain on closed field lines. *Rostoker and Samson* [1981] also suggest that the Harang discontinuity is the energy source region for the Pi 2. *Samson and Harrold* [1983], using the University of Alberta magnetometer chain, found that within the WTS the Pi 2 polarization patterns are clockwise (CW) as viewed downward. On the other hand, *Lester et al.* [1984] found with the mid-latitude Air Force Geophysics Laboratory (AFGL) chain, at the same longitude but equatorward, that the polarization ellipticity is predominantly counterclockwise (CC). These results are consistent with the fact that equatorward and poleward of the WTS the polarizations are counterclockwise while far to the east and west of the WTS they are CW. The Pi 2 polarizations relative to the WTS are therefore quite complex.

Paper number 5A8793
0148-0227/86/005A-8793$05.00

Causes of the observed east-west north-south transitions in the Pi 2 polarizations are an open question. According to *Pashin et al.* [1982], the Pi 2 current system is primarily located in the upward current at the surge head, and the westward movement of the surge causes linearly polarized Alfvén waves to appear elliptically polarized on the ground. *Samson* [1982], on the other hand, explains the observed polarization patterns in terms of a longitudinal distribution of oscillating current sheets. *Lester et al.* [1983, 1984] interpret the mid-latitude Pi 2 pulsations as arising from the field-aligned currents that form the substorm current wedge. *Ellis and Southwood* [1983] have examined the reflection of Alfvén waves from ionospheres with a discontinuity in either the Hall or the Pedersen conductivity. The reflection properties of the Alfvén wave depend not only on the discontinuity type but also on the orientation of the incident electric field vector. In two of the four cases studied, the field-aligned current sheets act as subsidiary surface waves centered on the field lines connected to the discontinuity. The subsidiary waves are circularly polarized and suppress any net flow of Hall current across the discontinuity. *Glassmeier* [1984] has extended the work of Ellis and Southwood to include arbitrary distributions in the height-integrated conductivity. Recently, *Southwood and Hughes* [1985] have suggested that two oppositely traveling east-west surface waves parallel to the conductivity gradients could give a combined signal that reproduces many of the observed features of the Pi 2 pulsations. An important unresolved question is the relation of the Pi 2 current system to the overall current system that forms the substorm current wedge.

It is assumed that the initial diversion of the cross-tail current is carried by a transverse Alfvén wave [*Baumjohann and Glassmeier*, 1984]. The subsequent reflection of the wave [*Maltinckrodt and Carlson*, 1978; *Nishida*, 1979; *Kan et al.*, 1982] between the conjugate ionospheres and the triggering of secondary Alfvén waves in the ionosphere [*Maltsev et al.*, 1974;

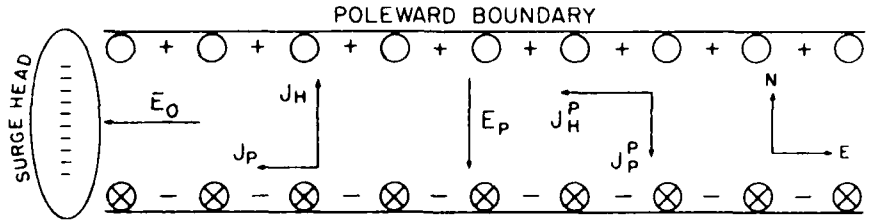

Fig. 1. Idealized model of the WTS as proposed by *Inhester et al.* [1981]. The total external electric field E_0 drives a westward Pedersen and a northward Hall current. If the northward Hall current is not fully continued by field-aligned currents into the magnetosphere, polarization charges build up on the poleward surge boundary, producing a southward directed electric field E_p. This southward electric field produces a Hall current in the same direction as the Pedersen current from the original electric field E_0.

Tamao and Miura, 1982] both contribute to the Pi 2 pulsation time profile. As pointed out by *Baumjohann and Glassmeier* [1984], it is important to treat the ionosphere as an active part of the ionosphere-magnetospheric coupling rather than just a reflecting boundary.

The purpose of this paper is to relate Pi 2 pulsations to the dynamics of the westward traveling surge (WTS). A dynamical surge model has been developed by *Rothwell et al.* [1984] using the Inhester-Baumjohann [*Inhester et al.*, 1981; *Baumjohann*, 1983] representation. Here the feedback instability analysis [*Sato and Holzer*, 1973; *Holzer and Sato*, 1973; *Sato*, 1982] is applied to the Inhester-Baumjohann model of the WTS used by *Rothwell et al.* [1984], hereinafter called paper 1. The equations are linearized in the standard fashion, and it is shown that the zero-order terms recover the poleward motion of the surge boundary as derived in paper 1. The first-order terms give rise to a dispersion relation for the feedback instability. This relation is solved for the allowed frequencies and their associated growth rates. It is found that the number of frequencies generated is related to the speed of the WTS boundaries. The resulting composite pulse shapes are shown to be very similar to those measured by *Singer et al.* [1985] at mid-latitudes. The physical picture presented is that the initial precipitation caused by the onset in the magnetotail triggers the feedback instability in the coupled ionosphere-magnetospheric system, thereby producing Pi 2 pulsations [*Baumjohann and Glassmeier*, 1984]. In the next section we relate the feedback instability to the Inhester-Baumjohann WTS model.

The Inhester-Baumjohann Model and the Feedback Instability

The Inhester-Baumjohann model is shown in Figure 1. A uniform westward electric field E_0 produces a northward Hall current that closes into the magnetosphere via field-aligned currents along the poleward surge boundary. If the precipitation is insufficient to close off this Hall current, then an effective polarization charge builds up along the conductivity gradient, producing a southward directed electric field. This electric field creates a southward Pedersen current opposite to the original Hall current and a westward Hall current that adds to the original westward Pedersen current driven by E_0.

As noted above, the Pi 2 current system and the substorm current system inside the wedge are not always the same. In this paper we initially assume that both current systems are colocated, which is true approximately 65% of the time [*Lester et al.*, 1983].

The feedback instability [*Ogawa and Sato*, 1971; *Sato and Holzer*, 1973] has its foundation in earlier work by *Atkinson* [1970]. The feedback instability was originally developed for the quiet arc, which has a much larger extension in the east-west direction than in the north-south direction, similar to the surge region. A downward field-aligned current on the equatorward edge of the arc closes via a northward Pedersen current to an upward field-aligned current on the poleward boundary. According to *Atkinson* [1970] a local ionospheric conductivity enhancement causes a local decrease of the electric field. The resulting divergence of the magnetospheric polarization currents produces precipitation that increases the original conductivity enhancement. If one visualizes a north-south ionospheric wave in the model in Figure 1, then one will have periodic conductivity enhancements which could lead to multiple arcs. The analysis for the quiet arcs as given by *Sato and Holzer* [1973] and *Holzer and Sato* [1973] is similar to the analysis presented here. In their analysis, active and passive ionospheric regions are conjugately connected by the same field line. The active ionosphere acts as an ac generator which produces an Alfvén wave that is damped in the passive ionosphere. *Sato* [1978, 1982] dispensed with the conjugately connected active and passive ionospheres and required that the Alfvén waves reflect upon reaching the equatorial plane. *Sato* [1978] also notes that the theory of quiet arcs must be self-consistent with the presence of a westward electric field. This is also a feature of the WTS as seen in Figure 1.

The feedback instability works because electrons tend to flow toward the positive part of the potential perturbation along the field lines. The inductive reactance of the magnetosphere, however, causes a phase lag in the precipitation such that it adds to the original ionization enhancement, causing the instability to grow. Should the magnetosphere have a capacitative reactance, then the precipitating electron flux coincides with the valley of the density distribution, and the perturbation decays. The magnetosphere must have an inductive response for the feedback instability to occur. By inductive and capacitative reactance we refer to the effective terminated transmission line impedance for Alfvén waves along the magnetic field lines [*Sato*, 1982]. This work has been extended by *Miura and Sato* [1980] to the global formation of multiple auroral arcs.

Tamao and Miura [1982], *Miura et al.* [1982], and *Tamao* [1984] considered a nonuniform magnetosphere coupling to the ionosphere. Negative Joule dissipation in the ionosphere is accompanied by a growing oscillation and an outflowing Poynting flux from the ionosphere. Damped oscillations occur when energy is supplied from the magnetosphere to the ionosphere. A large-scale uniform electric field in the ionosphere is required to drive the growing instability.

In the present work the generation of Pi 2 pulsations is

considered as follows. The injection of hot electrons from the plasma sheet during a substorm onset initiates the feedback instability in the ionosphere-magnetosphere system. This assumption is based on the satellite observations of *Sakurai and McPherron* [1983] that the Pi 2 burst is superimposed on a dc shift in the azimuthal component of the magnetic field which is caused by field-aligned currents. From their Figure 18 the Pi 2 occurs at the beginning of the dc shift. The parallel (precipitating) current is therefore considered to be decomposable into ac and dc components. The dc component is the primary injection from the distant magnetotail, and the ac component arises from the initial injection transient and the feedback instability. It will be shown below that the number of modes that are stimulated is dependent on the energy of the zero-order precipitation. It is argued that the feedback instability does not reach the nonlinear stage examined by *Sato* [1978] and *Miura et al.* [1982] since the flux associated with $j_{\parallel}$ (dc) raises the ionization level within a time $\approx (\alpha_r N_0)^{-1}$, where α_r is the electron-ion recombination rate and N_0 is the zero-order ion density. After this time, electron-ion recombination dominates, and the composite pulsation decays.

Kan et al. [1982] consider the Pi 2 wave form to arise from the superposition of the reflected and incident Alfvén waves impinging on a passive ionosphere. They neglect polarization and Hall current effects. Here, on the other hand, we consider the natural modes arising from a self-consistent ionosphere-magnetosphere interaction (i.e., the feedback instability).

FORMULATION OF THE MODEL

In paper 1 [*Rothwell et al.*, 1984] the solutions to the time-dependent zero-order equations along the surge boundary conductivity gradients were solved. On the other hand, in *Sato*'s [1982] theory the zero-order enhanced ionization density N_0 is taken as constant in space and time, which is consistent with the Inhester-Baumjohann model inside the surge region.

In formulating the present Pi 2 pulsation model we first connect the magnetospheric transverse Alfvén wave with the ionospheric drift wave [*Tamao and Miura*, 1982]. The Alfvén wave is probably kinetic. However, the perpendicular scale lengths considered here are much larger than the ion gyroradius so that the Alfvén dispersion relation is essentially the same as in the MHD case. It is permissible, therefore, in the present context to use the MHD dispersion relation. An Alfvén wave carries parallel current which is related to the divergence of the transverse electric wave field by

$$Z_0 j_{\parallel} = \nabla \cdot E_{\perp} \tag{1}$$

where Z_0 is the characteristic impedance of an equivalent transmission line terminated at both ends by the impedance Z_0 and $j_{\parallel}$ is in the same direction as the ambient magnetic field B_0. It can be shown [see *Kan et al.*, 1982] that $j_{\parallel}$ and $\nabla \cdot E_{\perp}$ satisfy the transmission line equations. *Sato* [1982] used the transmission line analogy to impose the ionospheric and equatorial boundary conditions. As seen at the ionosphere, the magnetospheric impedance is given by

$$Z = iZ_0 \cot(\omega l / V_A) \tag{2}$$

where V_A is the magnetospheric Alfvén speed and l is the length of the field line between the ionosphere and the equator. This expression also assumes that $j_{\parallel}$ is zero at the equatorial plane. Z_0 is given by $\mu_0 V_A$. Then (1) holds at the ionosphere if Z in (2) replaces Z_0 in (1).

The northward ionospheric current component in the Inhester-Baumjohann model is given by

$$J_x = E_y \Sigma_H + E_x \Sigma_p \tag{3}$$

where Σ_H and Σ_p are the Hall an Pedersen conductivities, respectively, and E is the electric field. The conductivities are normalized to their zero-order values by

$$\begin{aligned} \Sigma_H &= \Sigma_{H0} N \\ \Sigma_p &= \Sigma_{p0} N \end{aligned} \tag{4}$$

where Σ_{H0} and Σ_{p0} are uniform inside the surge region and N is the height-integrated ionospheric ionization density normalized to the uniform density within the surge region [*Sato*, 1982]. Now we similarly have for the westward (y) current component

$$J_y = \Sigma_p E_y - \Sigma_H E_x \tag{5}$$

Equations (3), (4), and (5) are linearized as follows.

$$\begin{aligned} E_x &= E_{x0} + \bar{E}_x \\ E_y &= E_{y0} + \bar{E}_y \\ N &= 1 + \bar{N} \end{aligned} \tag{6}$$

where the values with overbars are of first order. E_{y0} is the primary electric field that drives the substorm current wedge, and E_{x0} is the primary north-south polarization electric field. Both E_{x0} and E_{y0} are assumed constant inside the surge region. Now the constancy of N_0 and E_0 inside the surge region implies that there is no net zero-order field-aligned current closing into the magnetosphere inside the surge. However, there is still a zero-order energetic electron precipitation that maintains the high conductivity inside the surge region. The current carried by the energetic electrons must be precisely balanced by a flux of upward flowing ionospheric electrons of lower energy. In this manner a high conductivity level is maintained with no net current closure. The divergence of J is given by

$$\nabla \cdot \bar{\mathbf{J}} = \mathbf{J}_0 \cdot \nabla \bar{N} + \Sigma_{p0} \nabla \cdot \bar{\mathbf{E}} + \Sigma_{H0} (\nabla \times \bar{\mathbf{E}})_z \tag{7}$$

where J_0 is the zero-order two-dimensional ionospheric current. The ionosphere is considered a source of transverse Alfvén waves so that $(\nabla \times E)_z = 0$ [*Maltzev et al.*, 1974] excludes magnetoacoustic waves in the ionosphere. The first-order field-aligned current density is given by

$$j_{\parallel} = -\nabla \cdot \bar{\mathbf{J}} = -\mathbf{J}_0 \cdot \nabla \bar{N} - \Sigma_{p0} \nabla \cdot \bar{\mathbf{E}} \tag{8}$$

We assume that the first-order current is being carried by hot electrons. Note that we have a coordinate system with the upward current as positive, which means that we have a minus sign in the following relation,

$$Z j_{\parallel} = -\nabla \cdot \bar{\mathbf{E}}_{\perp} \tag{9}$$

and upon combining (8) and (9) we have

$$j_{\parallel} = -\mathbf{J}_0 \cdot \nabla \bar{N} (1 - Z \Sigma_{p0}) \tag{10}$$

Now the first-order continuity equation gives us

$$\begin{aligned} \partial \bar{N} / \partial t &= -Qh j_{\parallel} / e N_0 - 2 \hat{\alpha}_r \bar{N} \\ \hat{\alpha} &= \alpha_r N_0 h \end{aligned} \tag{11}$$

where Qh is the height-integrated ion production efficiency

[*Rees*, 1963]. The insertion of (10) into (11) gives

$$\partial \bar{N} / \partial t = -\mathbf{V} \cdot \nabla \bar{N} (1 - Z\Sigma_{p0}) - 2\alpha \bar{N} \tag{12}$$

where the components of **V** are given by

$$\begin{aligned} V_x &= Qh\alpha V_d \\ V_y &= QhV_d[1 + R^2(1 - \alpha)]/R \end{aligned} \tag{13}$$

The parameter α is the closure parameter as defined in the paper by *Rothwell et al.* [1984], V_d is the $E \times B$ drift velocity taken as ≈ 0.25 km/s, and R is the ratio of the height-integrated Hall to Pedersen conductivities, which we take to be ≥ 3. These are the components of the surge velocity as derived by *Rothwell et al.* [1984] without the electron-ion recombination term. This velocity term was derived in (12) by noting that

$$QhJ_0/eN_0 = Qh\, eN_0(\boldsymbol{\Sigma} \cdot \mathbf{E}) \tag{14}$$

where $\Sigma \approx eN_0 B_0$ leads to equations (9) and (11) in the paper by *Rothwell et al.* [1984].

It is assumed in the usual manner that

$$\bar{N} \approx \exp[i(k_x x + k_y y - \omega t)] \tag{15}$$

where ω is considered complex ($\omega = \omega_r + i\omega_i$) and k is the wave vector for the ionospheric wave. Taking $X = \Sigma_{p0} Z_0 \cot[\omega_r l / V_A - n\pi]$, we have

$$-i\omega_r + \omega_i = -i\mathbf{V} \cdot \mathbf{k}(1 + iX)/(1 + X^2) - 2\alpha \tag{16}$$

which leads to

$$\omega_r = \mathbf{V} \cdot \mathbf{k}/(1 + X^2) \tag{17}$$

for the frequency dispersion and

$$\omega_i = \omega_r X - 2\sigma_r N_0 \tag{18}$$

for the growth rate.

Sato [1978, 1982] has argued that the maximum growth rate occurs for $X = 1$. However, X is not a free parameter, and its value must be consistent with the solutions to (17). For each value of n ($n = 0, 1, 2, \cdots$) one obtains two solutions to (17). One root corresponds to a negative transmission line impedance or a capacitative reactance and is highly damped. The other root corresponds to a positive (inductive) reactance and gives positive growth. This result is consistent with the views of *Sato* [1978]. In the following discussion we consider only the inductive roots of ω_r.

One can view the substorm current wedge as forming a box shaped region of enhanced conductivity. The ionospheric waves associated with the Pi 2 pulsations partially reflect off the conductivity gradients on the boundaries forming standing waves in the x and y directions. In the following calculations it is assumed that the waves are dominated by the fundamental modes, i.e., the wavelengths in each component are of the same order as the scale size in that direction.

Now the $\mathbf{k} \cdot \mathbf{V}$ term in (17) can be expressed as (see (13))

$$W = \lambda_y \mathbf{k} \cdot \mathbf{V}/(2\pi QHV_d) = \{\gamma\alpha + [1 + R^2(1 - \alpha)]R\} \tag{19}$$

where $\gamma = \lambda_y/\lambda_x$, λ_y is the length of the surge wedge in the east-west direction, and λ_x is the surge width in the north-south direction. Figure 2 shows a plot of the right-hand side of (19) for various values of α and R. The long dashes in this figure represent the product $\gamma\alpha$. Note that for most cases, $\gamma\alpha$ is a reasonable approximation, which means that except for very small zero closures the north-south surge dimensions dominate the Pi 2 frequency characteristics. In the following example, therefore, we set λ_y to infinity and treat the north-south case. Note also that for larger α the Pi 2 pulsation frequencies are higher. The dependence of W and R is weak.

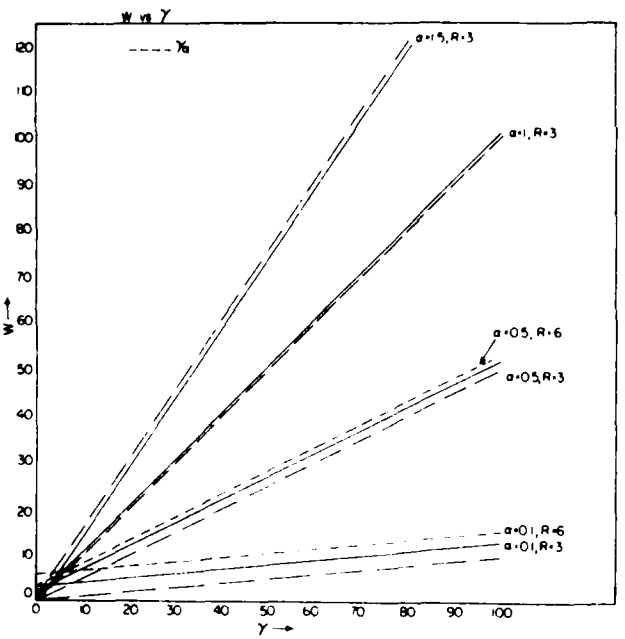

Fig. 2. The parameter W as defined in equation (19) in the text. This figure shows that except for almost zero closure ($\alpha = 0$) that $W = \gamma\alpha$ (denoted by solid lines) is a reasonable approximation. This graph indicates that the north-south surge dimensions generally determine the Pi 2 frequency characteristics.

As noted above, we solve for the inductive ($X > 0$) roots of (17). The resulting values of ω_r are inserted into the first term on the right-hand side of (18) and plotted in Figure 3*a*. The characteristic north-south dimension of the surge is taken as 500 km, and the quantities $\Sigma_0 Z_0$ and V_A/l are set to 10 and 0.005 s^{-1}, respectively. Note that a mode is excited whenever $X = 0$ or $\omega_r = (n + \frac{1}{2})\pi V_A/l$. This means that (17) has only physical solutions for frequencies less than $\pi V_x/\lambda_x$. Now the value of V_x increases with the energy of the precipitating electrons [*Rothwell et al.*, 1984]. Thus the energy of the zero-order component (dc) of the precipitating electrons controls the number of excited modes as seen from Figure 3*a*. More energetic precipitation is associated with higher magnetic activity. *Sakurai and McPherron* [1983] analyzed Pi 2 magnetic activity. *Sakurai and McPherron* [1983] analyzed Pi 2 magnetic pulsations observed at geosynchronous orbit on ATS 6. They found that as magnetic activity increased, the frequency spectrum became more complex with more spectral power at higher frequencies. This is consistent with Figure 3*a* in that a larger V_x is associated with more energetic electron precipitation and faster motion of the surge boundaries. As seen from Figure 3*a*, higher-frequency modes are excited at higher growth rates, implying a greater contribution to the spectral power. Figure 3*b* shows the corresponding mode frequencies for the same inputs as given for Figure 3*a*.

A horizontal line in Figure 3*a* would represent the damping due to electron-ion recombination. The net decay is the difference between this curve and the individual $\omega_r X$ curves. The present theory is applicable when the intersection of the V_x/λ_x line with the electron-ion loss rate is above the growth curves. If the intersection is below the growth curves, then continuous growth is predicted, which, of course, is unrealistic. Therefore this latter case should be treated by a more sophisticated non-

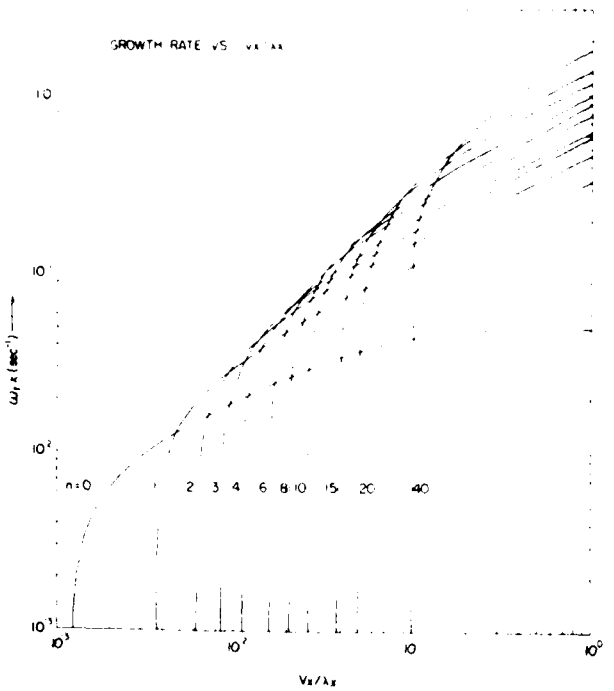

Fig. 3a. Growth rates for $\Sigma_p Z_0$ and $V_A/l = 0.005$. The north-south dimension of the surge, λ_x, is taken as 500 km. The growth rates $\omega_r X$ of the various excited frequency modes are plotted as a function of V_x/λ_x where V_x is the zero-order poleward surge velocity, neglecting electron-ion recombination effects. The value of this ratio determines the number of modes excited and the overall time profile of the resulting Pi 2 pulsation. A horizontal line equal to $2\sigma_r n$ would represent wave damping due to electron-ion recombination.

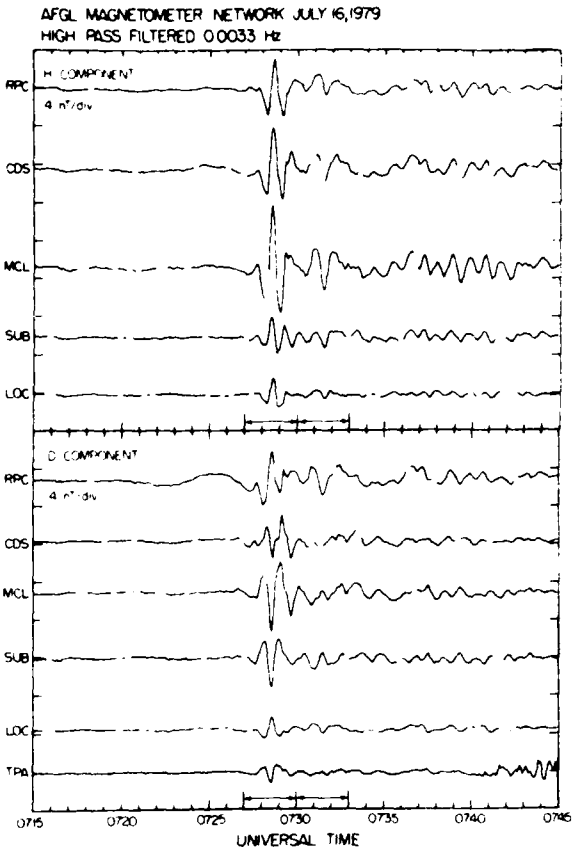

Fig. 4. AFGL magnetometer filtered Pi 2 data taken on July 16, 1979 (courtesy H. Singer AFGL).

linear approach. The sensitivity of the results to the various parameters is as follows. Higher electron precipitation energy implies that higher-order modes are excited with faster growth rates and also that a higher ionospheric ionization density is attained. These two effects tend to offset each other in the sense that a higher ionization level implies faster electron-ion recombination and hence enhanced damping. The faster growth rates dominate, however, so that the net effect is larger Pi 2 pulsations at higher incident electron energies. Higher incident flux at fixed incident energy can lead to overdamping. Lower flux causes more rapid growth. Smaller values of V_A/λ_x (longer field lines) lead to the excitation of more modes shifted to lower frequencies.

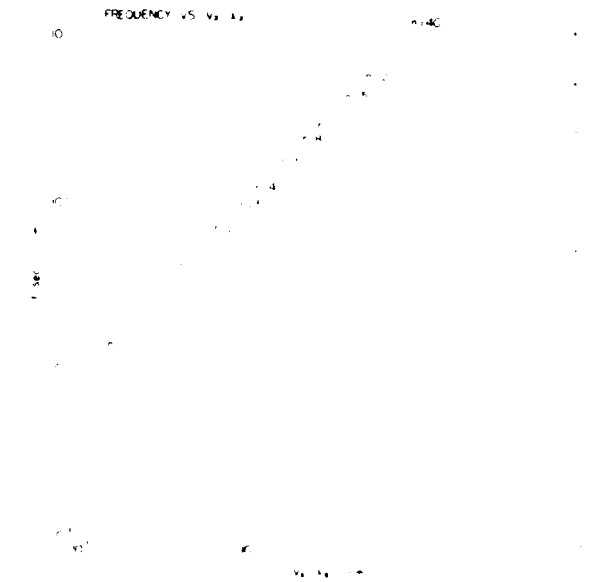

Fig. 3b. Frequencies of the various modes for the same input parameters as shown in Figure 3a.

In the present model an external condition is needed to relate the zero-order electron precipitation flux with the electron precipitation energy in order to ensure damped Pi 2 pulsations. We therefore took the results of *Fridman and Lemaire* [1980], who relate the field-aligned electron fluxes with the associated field-aligned potential drops. They consider five separate cases corresponding to different boundary conditions in the plasma sheet source. It was found that all five cases gave values for electron-ion recombination damping that were above the growth rate curves shown in Figure 3a. The *Fridman and Lemaire* [1980] results therefore are consistent with damped Pi 2 pulsations as derived from the present model.

Now in equation (23) of paper 1 we found that the incident flux along the poleward boundary had to exceed some critical value in order for the surge to propagate. It turns out that this critical flux exceeds the required flux level inside the surge region to cause damped Pi 2 pulsations. Therefore from the present work one expects damped Pi 2 pulsations associated with poleward surge movements. This is an important consistency test between our theoretical approach and observational results.

Figure 4 shows a Pi 2 pulsation as measured by *Singer et al.* [1985], and Figure 5 shows the results of the present calcula-

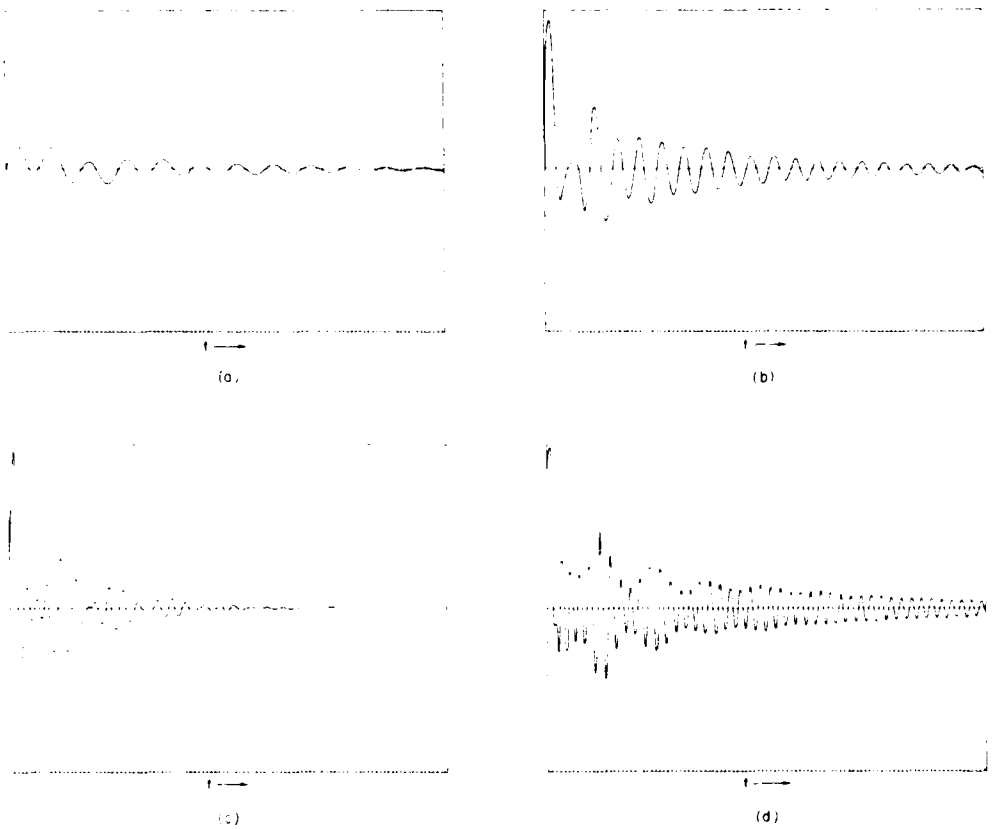

Fig. 5. The resulting model Pi 2 pulsation time profile based on the example shown in Figure 3*a*. This is a linear superposition of the individual modes assuming all are initially excited with an equal but arbitrary amplitude. Figures 5*a*–5*d* are the results for incident energies of 2 keV, 4 keV, 6 keV, and 8 keV, respectively. The corresponding precipitating electron fluxes used are 3.5×10^7, 7×10^7, 1.1×10^8, and 1.5×10^8 (cm^2 s)$^{-1}$. The equilibrium ionization level N_0 is given by $N_0 = (Q/\alpha_r)^{1/2}$ where Q is the ion production rate [*Rees*, 1963] and α_r is the electron-ion recombination rate. The damping term is given by $2\alpha_r N_0$ so that a minimum value of j is required in order to exceed the growth rates given in Figure 3*a*. Lower values of j lead to continued growth and to the nonlinear regime that is not covered in the present theory.

from where the excited modes were considered initialized at equal amplitudes and all having a sinusoidal dependence. The four cases (5*a*–5*d*) correspond to incident energies of 2 keV, 4 keV, 6 keV, and 8 keV. The incident electron fluxes used in Figures 5*a*–5*d* were 3.5×10^7, 7×10^7, 1.1×10^8, and 1.5×10^8 (cm^2 s)$^{-1}$, respectively. Note that the higher-frequency pulsations occur at higher incident energies. The agreement with *Singer et al.*'s [1985] data is seen to be quite good for Figure 5*c*. The other cases (particularly Figures 5*b* and 5*d*) are not inconsistent with observations, although they are a little too regular and last too long. A slight increase in ionization (electron precipitation flux) would significantly decrease the pulsation duration. It is concluded that the different damping rates for the frequencies arising from the Sato formulation can lead to composite pulses which are very similar to the measured Pi 2 pulsations in shape and time duration. Therefore ionospheric generation of Alfvén waves could provide the primary signature for Pi 2 pulsations. The damping of the Pi 2's is very sensitive to increases in the precipitation current that enhances N_0.

The resulting physical model is as follows. The interruption [illegible] dusk current in the plasma sheet causes electron [illegible] flux tubes to a more dipolar [illegible] formation of a substorm current wedge through the ionosphere. The impact of the initial precipitation [illegible] on the ionosphere triggers the feedback instability which has as a free energy source the east-west electric field E_{0y} in the substorm current wedge. The feedback instability fills the flux tubes from the ionosphere with Alfvén waves which form standing waves between conjugate ionospheres. Since the injected electrons are presumably on closed field lines, there is a simultaneous launching of Alfvén waves into the magnetosphere from comparable locations in the two ionospheres. The ionospheric conductivity is high inside the surge so that waves once injected into the magnetosphere are efficiently trapped between the conjugate ionospheres [*Hughes and Southwood*, 1976]. How do these standing Alfvén waves decay?

Sakurai and McPherron [1983] note Pi 2 polarization reversals in space similar to those observed by ground-based stations. They also point out that Pi 2's in space have a large compressional component and therefore can propagate across field lines as fast-mode hydromagnetic waves [*Singer et al.*, 1983]. The propagation speed is faster than the Alfvén speed since the fast-mode phase velocity is given as [*Akhiezer et al.*, 1975]

$$V_f = (V_A^2 + C_s^2)^{1/2} \tag{20}$$

where C_s is the sound speed. It is argued that these waves still have a velocity component parallel to the magnetic field so that they impinge on the ionosphere outside the surge region. Outside the surge, however, the ionospheric conductivity is

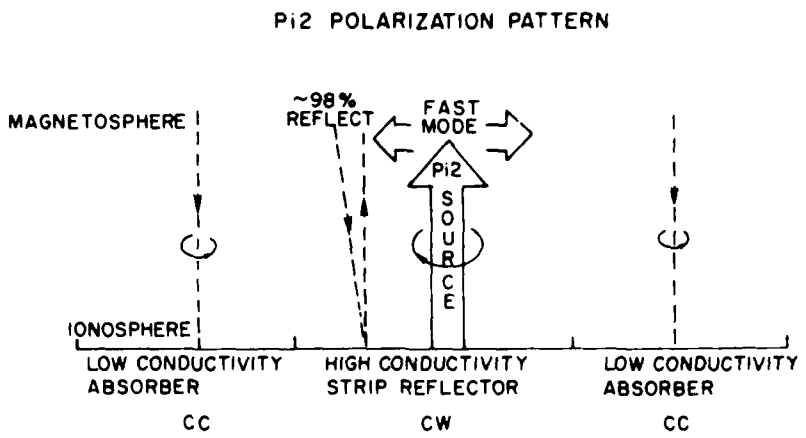

Fig. 6. Illustrates a possible explanation for the different Pi 2 polarization observed inside and outside the substorm current wedge. An incident Alfvén wave from the magnetosphere stimulates the feedback instability, as described in the text. The substorm wedge acts as an ionospheric source for Pi 2 pulsations with clockwise polarization. Farther out in the magnetosphere these couple to compressional waves that propagate perpendicular to B. Outside the substorm wedge region these compressional waves couple to Alfvén waves that are easily absorbed by the ionosphere in regions of low conductivity. As viewed from the ionosphere, these incident waves will have counterclockwise polarization consistent with observations.

much lower, and therefore wave reflection is much less efficient [*Hughes and Southwood*, 1976; *Ellis and Southwood*, 1983]. The magnetospheric Alfvén waves in these regions are rapidly damped by Joule heating [*Hughes and Southwood*, 1976].

The Alfvén wave created by the Sato feedback instability originates in the ionosphere and propagates into the magnetosphere. This wave is assumed to have clockwise polarization looking into the wave or counterclockwise polarization looking in the direction of propagation. It is also assumed that the sense of polarization is not affected by cross-field propagation via the fast-mode hydromagnetic wave. In the low-conductivity region outside the substorm current wedge the incident counterclockwise wave impinges on the ionosphere *from the magnetosphere*. If most of the incident wave in this region is absorbed by the ionosphere, then the polarization looking down is counterclockwise. In the high-conductivity region the launched waves are reflected in the conjugate ionosphere and return to the source region where they are highly reflected. Therefore the sense of polarization in the highly conductive region is determined by the ionospheric source characteristic of the feedback mechanism rather than by waves impinging from the magnetosphere. These concepts are illustrated in Figure 6.

In summary, the sense of polarization for ionospheric sources and sinks of Alfvén waves looking down at the ionosphere should be reversed. This interpretation is consistent with the observations of *Samson and Harrold* [1983] as described in the introduction.

The model has the following features.

1. The Pi 2 burst is a result of the sudden diversion of the tail current to the ionosphere [*Sakurai and McPherron*, 1983].

2. The feedback instability is an ionospheric source for Alfvén waves. Larger-amplitude components are generated at higher frequencies for more energetic precipitation.

3. Standing Alfvén waves are created between conjugate ionospheres on field lines that connect the source locations. These standing waves propagate across B field lines via fast-mode hydromagnetic waves. Outside the surge region the waves are rapidly damped in the regions of lower ionospheric conductivity. This model therefore provides a possible energy path that Pi 2 pulsations could follow.

4. The present model is consistent with the results of paper 1 [*Rothwell et al.*, 1984] in that the electron precipitation fluxes required for surge propagation are also sufficiently high to damp the excited Pi 2 pulsations. The flux levels predicted by *Fridman and Lemaire* [1980] also ensure the presence of damped Pi 2 pulsations in the model given here.

The present work does not exclude the possibility of additional magnetospheric sources of Pi 2 pulsations. We assume, however, that these Pi 2's are easily reflected by the high-conductivity region and that the ground-based magnetometers most efficiently respond to the ionospheric source presented here.

Acknowledgments. We would like to acknowledge the many useful and insightful comments by Carl-Gunne Fälthammar and Göran Marklund of the Royal Institute of Technology, Stockholm, Sweden, and by W. J. Burke, Howard Singer, and Michael Heineman at AFGL.

References

Akhiezer, A. I., I. A. Akhiezer, R. V. Polovin, A. G. Sitenko, and K. N. Stepanov, *Plasma Electrodynamics*, vol. 1, *Linear Theory*, translated from Russian by D. ter Haar, Pergamon, New York, 1975.

Atkinson, G., Auroral arcs: Result of the interaction of a dynamic magnetosphere with the ionosphere, *J. Geophys. Res.*, *75*, 4746–4754, 1970.

Baumjohann, W., Ionospheric and field-aligned current systems in the auroral zone: A concise review, *Adv. Space Res.*, *2*, 55–62, 1983.

Baumjohann, W., and K.-H. Glassmeier, The transient response mechanism and Pi2 pulsations at substorm onset: Review and outlook, *Planet. Space Res.*, *32*, 1361–1370, 1984.

Ellis, P., and D. J. Southwood, Reflection of Alfvén waves by non-uniform ionospheres, *Planet. Space Sci.*, *31*, 107–111, 1983.

Fridman, M., and J. Lemaire, Relationships between auroral electron fluxes and field-aligned electric potential differences, *J. Geophys. Res.*, *85*, 664–670, 1980.

Glassmeier, K.-H., On the influence of ionospheres with non-uniform conductivity distribution on hydromagnetic waves, *J. Geophys.*, *54*, 125–137, 1984.

Holzer, T. E., and T. Sato, Quiet auroral arcs and electrodynamic coupling between the ionosphere and magnetosphere, 2, *J. Geophys. Res.*, *78*, 7330–7339, 1973.

Hughes, W. J., and D. J. Southwood, The screening of micropulsation signals by the atmosphere and ionosphere, *J. Geophys. Res.*, *81*, 3234–3240, 1976.

Inhester, B. W., W. Baumjohann, R. W. Greenwald, and E. Nielsen, Joint two-dimensional observations of ground magnetic and ionospheric electric fields associated with auroral zone currents, 3, Auroral zone currents during the passage of a westward traveling surge, *J. Geophys.*, *49*, 155–162, 1981.

Kan, J. R., D. U. Longenecker, and J. V. Olson, A transient response model of Pi2 pulsations, *J. Geophys. Res.*, *87*, 7483–7488, 1982.

Lester, M., W. J. Hughes, and H. J. Singer, Polarization patterns of Pi2 pulsations and the substorm current wedge, *J. Geophys. Res.*, *88*, 7958–7966, 1983.

Lester, M., W. J. Hughes, and H. J. Singer, Longitudinal structure in Pi2 pulsations and the substorm current wedge, *J. Geophys. Res.*, *89*, 5489–5494, 1984

Mallinckrodt, A. J., and C. W. Carlson, Relations between transverse electric fields and field-aligned currents, *J. Geophys. Res.*, *83*, 1426–1432, 1978.

Maltzev, Yu. P., S. V. Leontzev, and W. B. Lyatsky, Pi2 pulsations as a result of evolution of an Alfven impulse originating in the ionosphere during a brightening of aurora, *Planet. Space Sci.*, *22*, 1519–1533, 1974.

Miura, A., and T. Sato, Numerical simulation of global formation of auroral arcs, *J. Geophys. Res.*, *85*, 73–91, 1980.

Miura, A., S. Ohtsuka, and T. Tamao, Coupling instability of the shear Alfvén wave in the magnetosphere with the ionospheric ion drift wave, 2, Numerical analysis, *J. Geophys. Res.*, *87*, 843–851, 1982.

Nishida, A., Possible origin of transient dusk-to-dawn electric field in the nightside magnetosphere, *J. Geophys. Res.*, *84*, 3409–3412, 1979.

Ogawa, T., and T. Sato, New mechanism of auroral arcs, *Planet. Space Sci.*, *19*, 1393–1412, 1971.

Pashin, A. B., K.-H. Glassmeier, W. Baumjohann, O. M. Raspopov, A. G. Yahnin, H. J. Opgenoorth, and R. J. Pellinen, Pi2 magnetic pulsations, auroral breakups, and the substorm current wedge: A case study, *J. Geophys.*, *51*, 223–233, 1982.

Rees, M. H., Auroral ionization and excitation by incident electron energetic electrons, *Planet. Space Sci.*, *11*, 1209–1218, 1963.

Rostoker, G., and J. C. Samson, Polarization characteristics of Pi2 pulsations and implications for their source mechanisms: Location of source regions with respect to the auroral electrojets, *Planet. Space Sci.*, *29*, 225–247, 1981.

Rothwell, P. L., M. B. Silevitch, and L. P. Block, A model for the propagation of the westward traveling surge, *J. Geophys. Res.*, *89*, 8941–8948, 1984

Sakurai, T., and R. L. McPherron, Satellite observations of Pi 2 activity at synchronous orbit, *J. Geophys. Res.*, *88*, 7015–7027, 1983.

Samson, J. C., Pi 2 pulsation: High latitude results, *Planet. Space Sci.*, *30*, 1239–1247, 1982.

Samson, J. C., and B. G. Harrold, Maps of the polarizations of high-latitude Pi 2's, *J. Geophys. Res.*, *88*, 5736–5744, 1983.

Samson, J. C., and G. Rostoker, Polarization characteristics of Pi2 pulsations and implications for their source mechanism: Influence of the westward travelling surge, *Planet. Space Sci.*, *31*, 435–458, 1983.

Sato, T., A theory of quiet auroral arcs, *J. Geophys. Res.*, *83*, 1042–1048, 1978.

Sato, T., Auroral physics, in *Magnetospheric Plasma Physics*, edited by A. Nishida, D. Reidel, Boston, Mass., 1982.

Sato, T., and T. E. Holzer, Quiet auroral arcs and electrodynamic coupling between the ionosphere and magnetosphere, 1, *J. Geophys. Res.*, *78*, 7314–7329, 1973.

Singer, H. J., W. J. Hughes, P. F. Fougere, and D. J. Knecht, The localization of Pi 2 pulsations: Ground-satelliteobservations, *J. Geophys. Res.*, *88*, 7029–7036, 1983.

Singer, H. J., W. J. Hughes, C. Gelpi, and B. G. Ledley, Magnetic disturbances in the vicinity of synchronous orbit and the substorm current wedge: A case study, *J. Geophys. Res.*, *90*, 9583–9589, 1985.

Southwood, D. J., and W. J. Hughes, Concerning the structure of Pi 2 pulsations, *J. Geophys. Res.*, *90*, 386–392, 1985.

Tamao, T., Magnetosphere-ionosphere interaction through hydromagnetic waves, Achievements of the International Magnetospheric Study (IMS), *Eur. Space Agency Spec. Publ., ESA SP-217*, 427–436, 1984.

Tamao, T., and A. Miura, Coupling instability of the shear Alfvén wave in the magnetosphere with the ionospheric ion drift wave, 1, Energetic consideration, *J. Geophys. Res.*, *87*, 905–911, 1982.

L. P. Block, Department of Plasma Physics, Royal Institute of Technology, Stockholm S 10044, Sweden.

P. L. Rothwell, Air Force Geophysics Laboratory/PHG, Hanscom Air Force Base, MA 01731.

M. B. Silevitch, Department of Electrical Engineering, Northeastern University, Boston, MA 02115.

(Received July 24, 1985;
revised November 18, 1985;
accepted November 18, 1985.)

END

DATE

FILMED

DTIC

JULY 88